Gastroenterology 2015;149:765–776

Complement Component 5 Mediates Development of Fibrosis, via Activation of Stellate Cells, in 2 Mouse Models of Chronic Pancreatitis

Matthias Sendler,[1,*] **Georg Beyer**,[1,*] Ujjwal M. Mahajan,[1] Vivien Kauschke,[1] Sandrina Maertin,[1] Claudia Schurmann,[2] Georg Homuth,[2] Uwe Völker,[2] Henry Völzke,[3] Walter Halangk,[4] Thomas Wartmann,[4] Frank-Ulrich Weiss,[1] Peter Hegyi,[5,6] Markus M. Lerch,[1,§] and Julia Mayerle[1,§]

[1]Department of Medicine A, [2]Interfaculty Institutes for Genetics and Functional Genomics, [3]Institute for Community Medicine, University Medicine, Ernst-Moritz-Arndt University, Greifswald, Germany; [4]Department of Surgery, Division of Experimental Surgery, Otto-von-Guericke University, Magdeburg, Germany; [5]First Department of Medicine, University of Szeged, Szeged, Hungary; [6]MTA-SZTE Lendulet Translational Gastroenterology Research Group, Szeged, Hungary

BACKGROUND & AIMS: Little is known about the pathogenic mechanisms of chronic pancreatitis. We investigated the roles of complement component 5 (C5) in pancreatic fibrogenesis in mice and patients. **METHODS:** Chronic pancreatitis was induced by ligation of the midpancreatic duct, followed by a single supramaximal intraperitoneal injection of cerulein, in C57Bl6 (control) and C5-deficient mice. Some mice were given injections of 2 different antagonists of the receptor for C5a over 21 days. In a separate model, mice were given injections of cerulein for 10 weeks to induce chronic pancreatitis. Direct effects of C5 were studied in cultured primary cells. We performed genotype analysis for the single-nucleotide polymorphisms rs 17611 and rs 2300929 in *C5* in patients with pancreatitis and healthy individuals (controls). Blood cells from 976 subjects were analyzed by transcriptional profiling. **RESULTS:** During the initial phase of pancreatitis, levels of pancreatic damage were similar between C5-deficient and control mice. During later stages of pancreatitis, C5-deficient mice and mice given injections of C5a-receptor antagonists developed significantly less pancreatic fibrosis than control mice. Primary pancreatic stellate cells were activated in vitro by C5a. There were no differences in the rs 2300929 SNP between subjects with or without pancreatitis, but the minor allele rs17611 was associated with a significant increase in levels of *C5* in whole blood. **CONCLUSIONS:** In mice, loss of C5 or injection of a C5a-receptor antagonist significantly reduced the level of fibrosis of chronic pancreatitis, but this was not a consequence of milder disease in early stages of pancreatitis. C5 might be a therapeutic target for chronic pancreatitis.

Keywords: Pancreatic Stellate Cells; Transcriptome Analysis; Complement System; αSMA.

Chronic pancreatitis is an inflammatory disease of the pancreas. Periodic repetitive inflammatory events result in the replacement of exocrine and endocrine tissue by fibrotic or fatty tissue, which leads to the loss of pancreatic function.[1,2]

The activation of pancreatic stellate cells (PSCs) is critical for the formation of extracellular matrix and fibrosis.[3] PSCs are present in their quiescent phenotype in the healthy pancreas, but during pancreatic injury and inflammation they undergo activation. Major activators of PSCs include inflammatory mediators such as transforming growth factor β (TGFβ), tumor necrosis factor α (TNFα), or interleukin (IL)6,[4,5] as well as ethanol and its metabolites.[6] Stellate cells respond to these activators with an increased expression of α smooth muscle actin (αSMA); an excessive release of extracellular matrix proteins such as collagen type I, III, or fibronectin; and increased cell proliferation.[5,7] Hepatic stellate cells (HSCs), which are related closely to PSCs,[8] have a similar activator profile.[9]

Preliminary data have suggested a critical role of complement factor 5 (C5) in liver fibrosis. Mice deleted in *C5* show significantly reduced liver fibrosis upon CCl_4 treatment and the same phenotype was achieved by treatment with a C5a-receptor antagonist.[10] In mice, mutations of *C5* have been associated with liver fibrosis, and 2 single-nucleotide polymorphisms (SNPs) in human *C5* have been reported to increase the risk of fibrosis in patients with hepatitis C.[10,11] The biological role of *C5* mutations are discussed controversially because a second larger study could not reproduce the initial association.[12] However, *C5* mutations have not yet been studied in the context of chronic pancreatitis.

C5a is a cleavage product of C5, which is generated during the classic and the alternative pathways of complement activation. C5a is a potent chemoattractant for neutrophils and macrophages and directly acts on a number of parenchymal cells via binding to the C5a receptor (CD88).

*Authors share co-first authorship; §Authors share co-senior authorship.

Abbreviations used in this paper: **C5, complement component 5; HSC, hepatic stellate cell; IL, interleukin; IP, intraperitoneal; MPO, myeloperoxidase; PSC, pancreatic stellate cell; αSMA, α smooth muscle actin; SNP, single-nucleotide polymorphism; TGFβ, transforming growth factor β; TNFα, tumor necrosis factor α.**

Most current article

0016-5085
http://dx.doi.org/10.1053/j.gastro.2015.05.012

During pancreatitis the complement system undergoes activation and serum levels of anaphylatoxin (C5a) correlate with the severity of the disease.[13,14] Pancreatitis is characterized by premature activation of zymogenes within the acinar cells, which leads to autodigestion of the organ, resulting in a systemic inflammatory response. A crucial step in the activation cascade leading to autodigestion is the activation of trypsinogen by cathepsin B.[15] Trypsin is also a potent complement activator cleaving C3 and C5, which results in the release of C3a and C5a, the enzymatically active form.[16] These 2 aspects, the activation of C5 by trypsin during pancreatitis and the potential impact of C5a on fibrogenesis, suggest a critical role of C5a in the progression of chronic pancreatitis.

The aim of this study was to study chronic pancreatitis in 2 animal models mimicking the human disease and to investigate the role of C5 in the development of fibrosis and its potential as a therapeutic target. We also studied the effect of disease-relevant SNP genotypes and their association with the transcriptome in whole blood.

Materials and Methods

See the Supplementary Materials and Methods section for more detail. In brief, C57Bl6 mice were purchased from Charles River (Sulzfeld, Germany), breeder pairs of C5-deficient mice as well as C5 wild-type animals were purchased from Jackson Lab (Bar Harbor, Maine).[17] Chronic pancreatitis was induced by ligation of the pancreatic duct at the junction between the gastric and the duodenal lobe, sparing the bile duct and its concomitant artery in animals at the age of 8–10 weeks, weighing approximately 25 g (Figure 1*A*). The animals received a single intraperitoneal (IP) injection of cerulein (50 μg/kg/body weight) 2 days after duct ligation. Animals were killed 3, 7, 14, and 21 days after ligation. Inhibition of C5a receptor was performed by daily IP injections of C5a-receptor antagonist W-54011 (200 μg/kg/body weight; Calbiochem, San Diego, CA[18]) starting 4 days after duct ligation. The peptide inhibitor AcF-(OpdChaWR) as well as its inactive control peptide Acd-ChaPWFRO-NH_2 were synthesized by Biosyntan GmbH (Berlin, Germany) and injected daily intraperitoneally at a concentration of 10 μmol/L starting at day 4 after ligation.[19] Animals were killed 14 days after pancreatic duct ligation. As a second

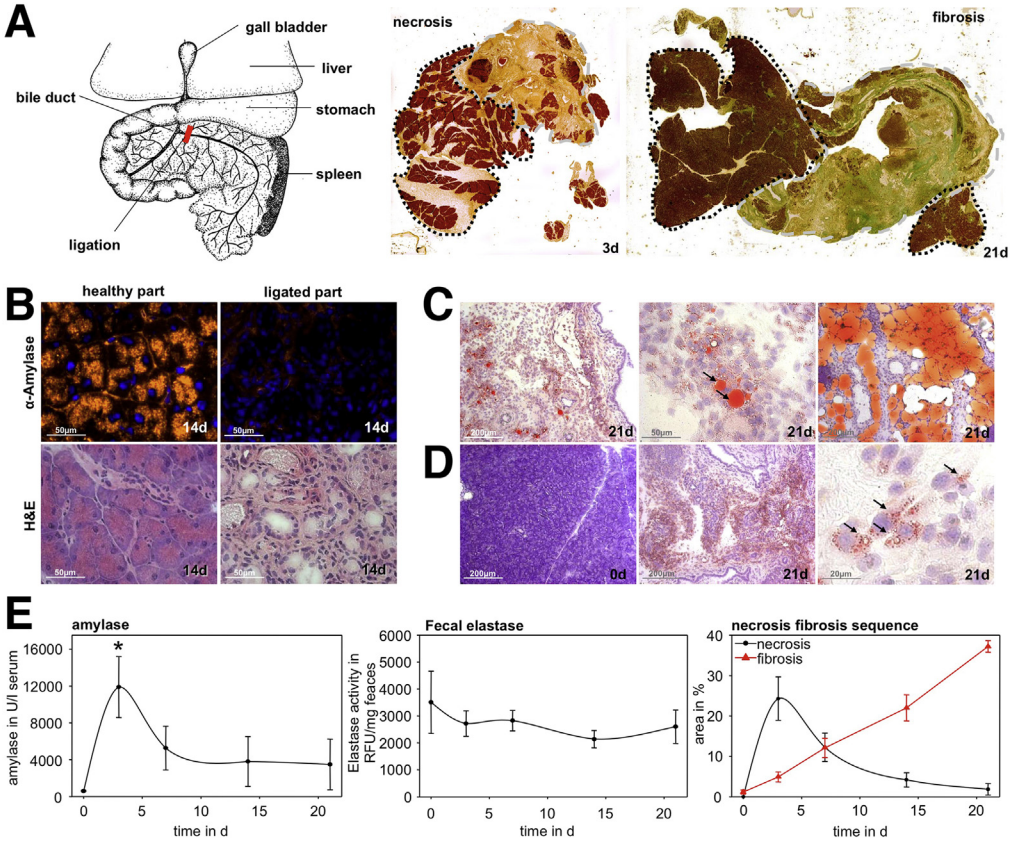

Figure 1. Characterization of combined duct ligation and supramaximal secretagogue stimulation to induce chronic pancreatitis in mice. Chronic pancreatitis was studied in C57BL6 mice using a combination of duct ligation and supramaximal secretagogue stimulation. In the mouse pancreas the common bile duct passes through the duodenal lobe of the pancreas and the side branches from the pancreatic head drain into the bile duct before reaching the papilla. (*A*) We therefore ligated the pancreatic duct at the junction between the duodenal, splenic, and gastric lobe. (*B*) The loss of exocrine tissue was shown by reduced amylase staining in the pancreas 14 days after duct ligation. (*C*) Fatty tissue replacement developed in the affected part of the pancreas, (*D*) some stellate cells show a positive oil red staining in small fat droplets. (*E*) Serum amylase level peaked at day 3. Loss of exocrine tissue was observed only in the disease-affected part, whereas overall exocrine function measured as fecal elastase activity was preserved. Quantification of necrosis on H&E staining and fibrosis in Masson–Goldner staining showed a necrosis-fibrosis sequence (n = 5–8).

chronic pancreatitis model we used 6 cerulein (50 μg/kg/body weight) IP injections twice a week over a time period of 10 weeks. Animals were killed 2 days after the last course of injection. All animal experiments were performed after prior institutional review board approval. More than 5 animals were used for each experiment and all experiments were performed in triplicate. All experiments were performed independently on 3 or more occasions. Asterisks indicate significant differences with a *P* value less than .05 and can be found on top of the graphs. The following antibodies were used for immunohistochemistry as well as immunofluorescence and were used as previously described: collagen-I (cat no. ab292; Abcam, Cambridge, United Kingdom), Ki67 (cat no. IHC-00375; Bethyl, Montgomery, TX), αSMA (clone 1A4; Sigma-Aldrich, Taufkirchen, Germany), anti–Mac-3 antibody (clone M3/84; BD Pharmingen, Heidelberg, Germany), and anti-myeloperoxidase (MPO) antibody (cat no. ab45977; Abcam, Cambridge, United Kingdom). Anti-protein gene product 9.5 (ref. Z5116; Dako, Hamburg, Germany), anti-insulin (4590; Cell Signaling, Leiden, The Netherlands), C5a receptor (CD88) (cat no. 135804; BioLegend, San Diego, CA) for IF and CD88 (cat no sc-25774; Santa Cruz Biotechnology, Dallas, TX) for IHC, CD68 (M1 macrophages), and CD206 (M2 macrophages) (antibody online cat no. ABIN181836 and cat no ABIN1386219, Aachen, Germany). Quantification of Goldner staining and immunohistochemistry was obtained using ImageJ software (National Institutes of Health, Bethesda, MD) (Supplementary Figure 1). Oil red staining was generated by the Oil-Red-O-Stain-Kit (IHC World, Woodstock, MD) and by Masson–Goldner staining using a kit from Merck (Darmstadt, Germany). Amylase, lipase concentrations, MPO, and Western blot of tissue or PSCs was performed as previously described.[20] Stellate cells were isolated from murine pancreas as described by Apte et al.[21] Blood samples from patients with pancreatitis and blood donors at our institution were collected after informed consent and ethics committee approval.[22] For SNP analysis only acute pancreatitis of a nonbiliary and non–endoscopic retrograde cholangiopancreatography–induced etiology, and for chronic disease only alcohol-induced or idiopathic pancreatitis, were included. TaqMan assays C_11720402_10 for the SNP rs17611 and C_2783669_1 for SNP rs2300929 was purchased from Life Technologies (Grand Island, NY). TaqMan products were verified by direct sequencing. The Study-of-Health-in-Pomerania is a longitudinal population-based cohort study in Western Pomerania.[23] The presented expression of quantitative trait loci analysis is based on a subset of 976 subjects.

Results

Ligation of the Gastric and Splenic Part of the Pancreatic Duct in Combination With Supramaximal Secretagogue Stimulation Leads to Chronic Pancreatitis With Significant Fibrosis and Loss of Exocrine Tissue

Chronic pancreatitis is characterized by a necrosis-fibrosis sequence.[24] The hallmark of the disease onset is characterized by the necrosis of acinar tissue. During pancreatic regeneration necrotic areas are replaced by extracellular matrix, resulting in extensive fibrosis. To study chronic pancreatitis in mice we used 2 models: first, using a combination of duct ligation and supramaximal cerulein (50 μg/kg/body weight) stimulation (Figure 1*A*), and, second, repetitive supramaximal (50 μg/kg/body weight) cerulein IP injections. To characterize the first model we analyzed pancreatic tissue on days 3, 7, 14, and 21 after surgery; animals who received only ligation of the pancreatic duct (Supplementary Figure 2*A*) as well as sham-operated animals served as controls (0 days). Ligation of the pancreatic duct followed by a single cerulein injection 2 days after surgery resulted in severe necrotizing pancreatitis in the ligated part of the pancreas, whereas the nonligated part was not affected 3 days after surgery (Figure 1*A*). Model-associated mortality ranged from 10% to 15% and always occurred within 48 hours of cerulein injection. Affected animals died from severe necrotizing pancreatitis and subsequent organ failure. Pancreatic necrosis was replaced by fibrotic tissue and maximal fibrosis was detected after 21 days (Figure 1*A*), as shown by the quantification of necrosis and fibrosis on histology (Figure 1*B* and *E*). Compared with the chronic pancreatitis model using repetitive cerulein injections over 10 weeks, the combination of duct ligation with a single cerulein injection lead to a significantly enhanced fibrosis reaction (Supplementary Figure 3*A* and *B*). In addition to the development of fibrosis, fatty tissue replacement in the pancreas was observed in the ligation model (Figure 1*C*). Oil red staining showed not only fatty tissue replacement, but also a significant number of PSC cells with small intracellular lipid droplets at 21 days after ligation (Figure 1*D*). Serum amylase (Figure 1*E*) as a marker for local pancreatic damage was increased significantly on day 3, but returned to normal on days 7, 14, and 21 after ligation (Figure 1*E*). The model reported here is characterized by a loss of digestive enzymes in the affected part of the pancreas (Figure 1*E*) and by a necrosis-fibrosis sequence (Figure 1*E*). Because only half of the pancreas is affected, animals do not develop overt exocrine (Figure 1*E*) or endocrine insufficiency (Supplementary Figure 4*C*).

To obtain a more detailed characterization of the mouse model a number of histologic stainings were performed. H&E staining illustrated the altered pancreatic morphology with initially large areas of necrosis and a pronounced inflammatory infiltrate. Over time, this was replaced by fibrotic tissue, degeneration of pancreatic acini, and a slowly decreasing inflammatory infiltrate resulting finally in scar tissue (Figure 2). Masson–Goldner trichrome staining allowed visualization of the extent of fibrogenesis (green) in the pancreas and the concomitant loss of exocrine tissue (red) over time in the ligated part of the pancreas (Figure 2). Immunohistochemical staining of the extracellular matrix proteins collagen-I and αSMA in pancreatic tissue indicated a similar trend by day 7, reaching its maximum 21 days after ligation (Figure 2). αSMA staining points to the activation of stellate cells, which is known to play a crucial role for pancreatic regeneration, fibrosis, and the production of extracellular matrix.[25] Ki67, a marker of proliferation, was detected mainly in inflammatory cells in the early disease phase but later also in the nuclei of acinar cells during organ regeneration (Figure 2). The acute phase of pancreatitis in this model was characterized by a massive infiltration of

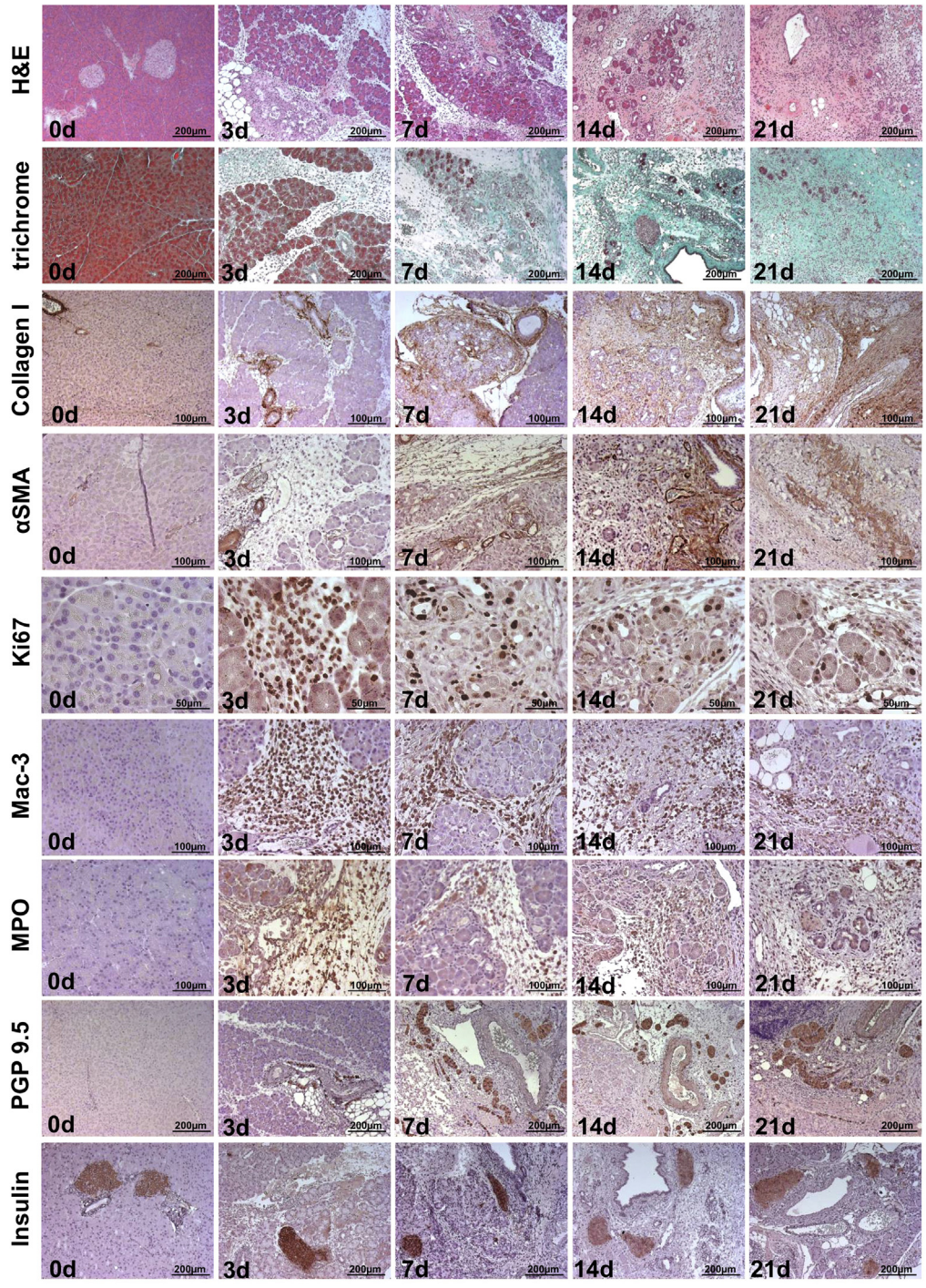

Figure 2. Morphologic characterization of the duct ligation model of chronic pancreatitis. The histologic characterization of pancreatic specimens in the duct ligation model of chronic pancreatitis showed typical features of chronic pancreatitis. H&E as well as Masson–Goldner staining showed a large increase in fibrosis. Immunohistochemical staining of collagen I and αSMA showed activation of PSCs and increased fibrogenesis with production of extracellular matrix proteins at 14 and 21 days after duct ligation. Pancreatic regeneration is marked by proliferating Ki67-positive acinar cells and tubular complexes 14 and 21 days after surgery. The transmigration of the innate immune cells was shown by Mac-3 staining for macrophages and MPO staining for neutrophils. Enlarged neural structures also were a common aspect of chronic pancreatitis, labeled here with protein gene product 9.5, suggesting neural sprouting. Insulin staining showed intact β-cells in islands of Langerhans (n = 5–8).

immune cells into the pancreas. Three days after pancreatic duct ligation macrophages as indicated by anti–Mac-3 staining (Figure 2) and neutrophils labeled with a MPO antibody (Figure 2) were found to transmigrate. Although initially the M1 population of macrophages was more prominent in the course of chronic pancreatitis, M2 macrophages prevailed at later time points (Supplementary Figure 4*D*). The systemic immune reaction was confirmed by increased serum IL6 levels and lung histology (Supplementary Figure 4*A* and *B*). In the chronic phase we detected nerve sprouting as another characteristic feature of chronic pancreatitis and the infiltration of immune cells toward these nerves that are thought to mediate neuropathic pain,[26] together with an increased nerve diameter in later stages of the disease as shown by protein gene product 9.5 (PGP 9.5) labeling (Figure 2).Open-field analysis of the animals to measure pancreatic pain confirmed this finding. Voluntary movement and the distance traveled by animals

in the duct-ligation model was decreased significantly in comparison with controls and animals after repetitive cerulein injections (Supplementary Figure 2*B*).

Chronic Pancreatitis in C5-Deleted Mice

We used the same 2 models (ligation with a single cerulein injection and repetitive IP cerulein) in C5-deficient (C5-/-) animals and their respective wild-type littermates (C5+/+).

Initially, we studied the systemic inflammation because C5 is a potent chemoattractant. MPO activity in lung tissue did not differ between the 2 animal strains, however, C5-deficient mice appeared to recruit higher numbers of neutrophils to the lungs (Figure 3*A*), but this trend did not reach statistical significance (Figure 3*B*). To

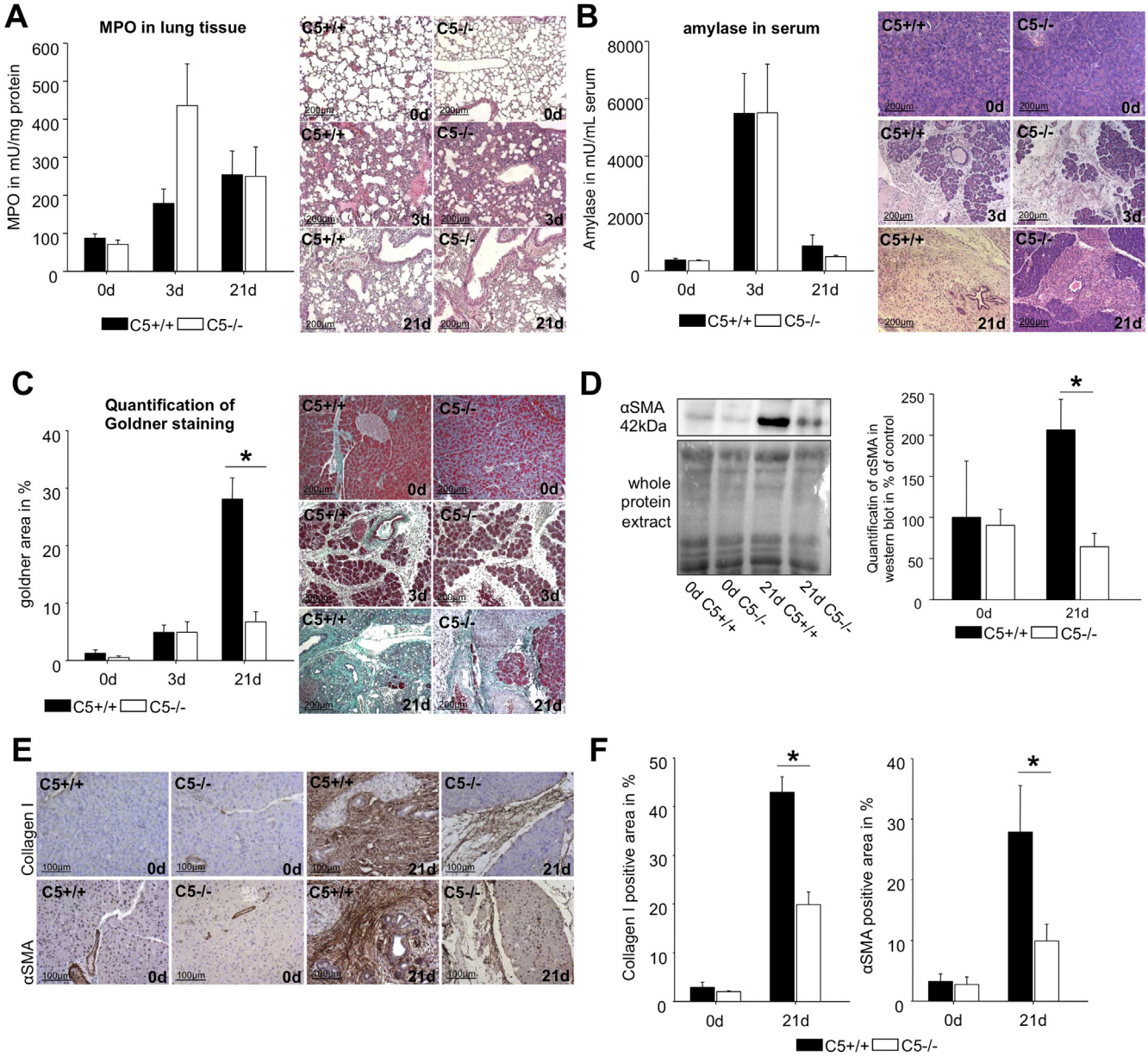

Figure 3. Course of chronic pancreatitis and extent of fibrogenesis in C5-/- and C5+/+ in the duct ligation model. (*A*) The systemic inflammatory reaction after induction of pancreatitis was illustrated by MPO activity measurements in lung tissue. Inflammation was confirmed by H&E staining of the lung. (*B*) There was no difference in serum amylase levels between animal strains. H&E staining of pancreatic tissue showed severe acute pancreatitis with large areas of necrosis 3 days after induction of pancreatitis. Twenty-one days after surgery necrotic areas were replaced by fibrotic tissue in C5+/+ but not in C5-/- animals. (*C*) The quantification of fibrosis showed a significant difference with regard to fibrogenesis between C5+/+ and C5-/- mice. (*D*) The expression of αSMA in the pancreas was reduced in C5-/- animals after 21 days. (*E* and *F*) In the more specific labeling for the extracellular matrix protein collagen I as well as αSMA C5-/- animals showed a less pronounced expression compared with C5+/+ mice (n = 5–10). Asterisks indicate significant differences with $P < .05$.

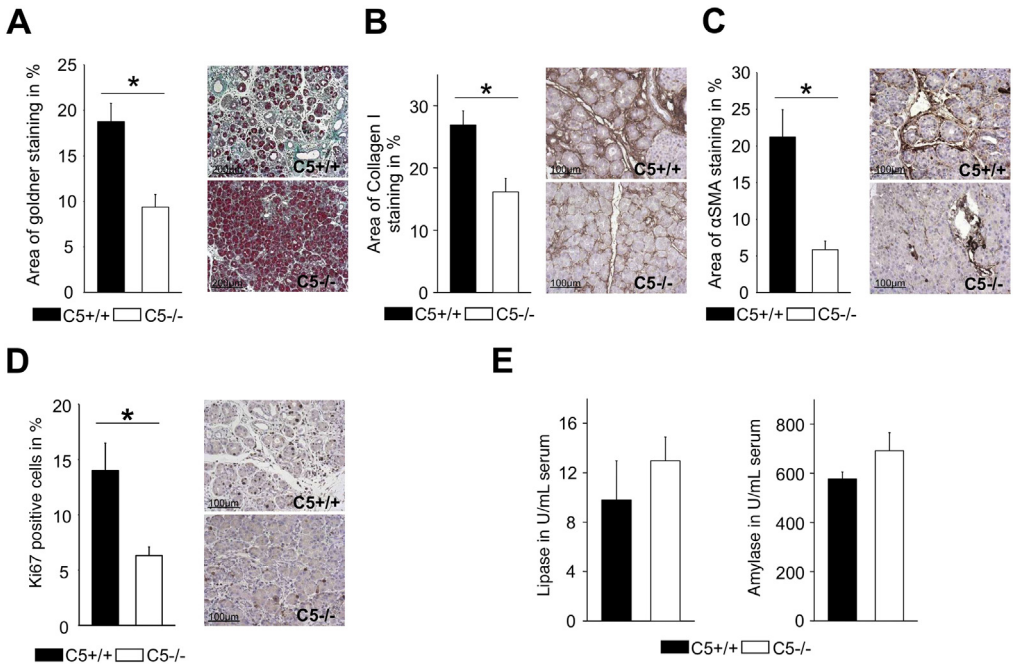

Figure 4. Extent of fibrogenesis in the course of chronic pancreatitis in C5-/- and C5+/+ animals in the model of repetitive cerulein stimulation. Masson–Goldner staining of pancreatic tissue was analyzed by ImageJ software (National Institutes of Health). (*A–C*) C5-deleted animals showed significantly less fibrosis in Masson–Goldner staining as well as αSMA and collagen I expression. (*D*) The percentage of Ki67-positive cells was reduced significantly in C5-/- animals, whereas (*E*) serum amylase and lipase activity were unaffected by C5 deletion (n = 5–7). Asterisks indicate significant differences with $P < .05$.

investigate differences during the severity of the disease in the initial phase, which might reflect on the chronification, we measured serum amylase concentrations at day 3 as well as 21 days after the onset of pancreatitis (Figure 3*B*). Both animal strains showed a significant increase in serum amylase activity but no differences were detected between the groups. Twenty-one days after induction of pancreatitis the serum amylase levels had decreased back to near baseline levels. Histology of the pancreas showed extensive necrotic areas in both animal strains (Figure 3*B*), which was replaced by fibrotic tissue in C5+/+ but not in C5-/- mice after 21 days. In both experimental models there was no difference in acute severity or initial necrosis between C5-deleted and wild-type animals (Supplementary Figure 5*A–D*). There was no difference in serum amylase or lipase activity, or for the infiltration of neutrophils as shown by pancreatic MPO activity between C5-/- and C5+/+ animals. The deletion of C5 did not affect severity or immune response during the early disease phase, confirming previous observations by Bhatia et al.[27]

Quantification of pancreatic fibrosis was performed by Masson–Goldner staining and immunohistochemistry was performed for collagen I and αSMA. All markers evaluated showed a significant reduction of fibrotic tissue in the C5-deleted animals (Figure 3*C–F*) in the ligation/cerulein injection model and were confirmed in the repetitive cerulein (10 weeks) injection model (Figure 4*A–D*). Again, markers for disease severity during the initial acute phase did not differ between the mouse strains (Figure 4*E*).

The observation that the absence of fibrosis in C5-deleted animals was independent of the differences in initial disease severity between C5+/+ and C5-/- mice (which was indistinguishable) suggests that C5 plays a direct role in fibrogenesis.

C5a Activates Pancreatic Stellate Cells

In resection specimens from chronic pancreatitis tissue of mouse and human pancreas we stained CD88-positive cells within the fibrotic tissue (Figure 5*A* and *B*) and confirmed the expression of CD88 on Western blot (Figure 5*B*). Furthermore, in murine pancreatic tissue we identified cells expressing αSMA and the C5a receptor (Figure 6*A*), suggesting that PSCs express the C5a receptor on their surface. By reverse-transcription polymerase chain reaction and on Western blot analysis we detected the expression of CD88 on freshly isolated PSCs in vitro (Figure 6*B* and *C*). Stimulation of PSCs with recombinant mouse C5a for 72 hours lead to significant up-regulation of αSMA expression. Stimulation with TGFβ as well as incubation with a C5a-receptor-1 inhibitor served as controls (Figure 6*C* and *D*). Real-time polymerase chain reaction analysis confirmed these findings and showed up-regulation of extracellular matrix proteins such as fibronectin, as well as αSMA (Figure 6*E*). PSCs of C5-/- mice showed no functional defects and responded in the same manner to TGFβ and C5a (data not shown). These experiments indicated a direct effect of C5a on PSC transdifferentiation to an activated, myofibroblast-like phenotype that synthesizes and secretes extensive amounts of extracellular matrix proteins.[3,28]

Inhibition of the C5a-Receptor-1 Protects Against the Development of Fibrosis in the Duct Ligation Model of Chronic Pancreatitis

Anti-C5 treatment of chronic pancreatitis was achieved by using 2 different inhibitors of the C5a-receptor-1 (CD88):

a small-molecule inhibitor (C5a-receptor antagonist) and a peptide inhibitor. Both inhibitors were used in a therapeutic approach starting 4 days after duct ligation. All markers of fibrosis (trichrome, collagen I, and αSMA) were reduced significantly by the C5a-receptor antagonist treatment compared with untreated pancreatitis animals. The peptide inhibitor directed against the C5a-receptor-1 was less effective compared with the small-molecule inhibitor, but also resulted in a trend toward reduced fibrosis (Figure 7*A*–*C*).

C5 SNPs Are Not Associated With an Increased Risk of Chronic Pancreatitis in Human Beings But With C5 Expression in a Population-Based Setting

Two common genetic polymorphisms have been described previously to be associated with an increased risk for developing liver fibrosis.[10,11] We therefore investigated whether these putative risk alleles, rs17611_A and rs2300929_T, are associated significantly with chronic pancreatitis. We genotyped these 2 SNPs in 390 chronic pancreatitis patients, 133 patients with acute pancreatitis, and 384 healthy blood donors and compared allele frequencies. No significant differences could be found between the groups (Supplementary Table 1), indicating that the 2 analyzed SNPs may not confer an individual risk for the development of chronic pancreatitis in patients with similar risk profiles. Patient characteristics are shown in Supplementary Table 2. However, a *cis*-expression of quantitative trait loci analysis of 976 volunteers from the Study of Health in Pomerania–Trend cohort showed a significant association of rs17611_A with increased *C5* expression in whole blood ($P = 6.87 \times 10^{-41}$ after adjustment for the first 50 principal components) (Supplementary Figure 6*A*). This indicates a correlation between C5-genotype and C5-protein expression. To show an association between C5 genotype variants and the risk of pancreatitis may require a much larger multicenter patient cohort.

Discussion

Chronic pancreatitis is burdened not only with a significant reduction in the quality of life of affected patients and an excess mortality, but also considerable health care costs.[1] Pancreatic fibrosis is a hallmark of the disease, but because of a lack of appropriate in vitro and in vivo models and because repeated tissue samples from patients are not available the underlying pathophysiological mechanisms of disease progression are poorly understood. Even in the 21st century we cannot offer a causal treatment to our patients or one that alters the natural history of pancreatic fibrosis. It is still unclear how fibrogenesis is initiated in the inflamed

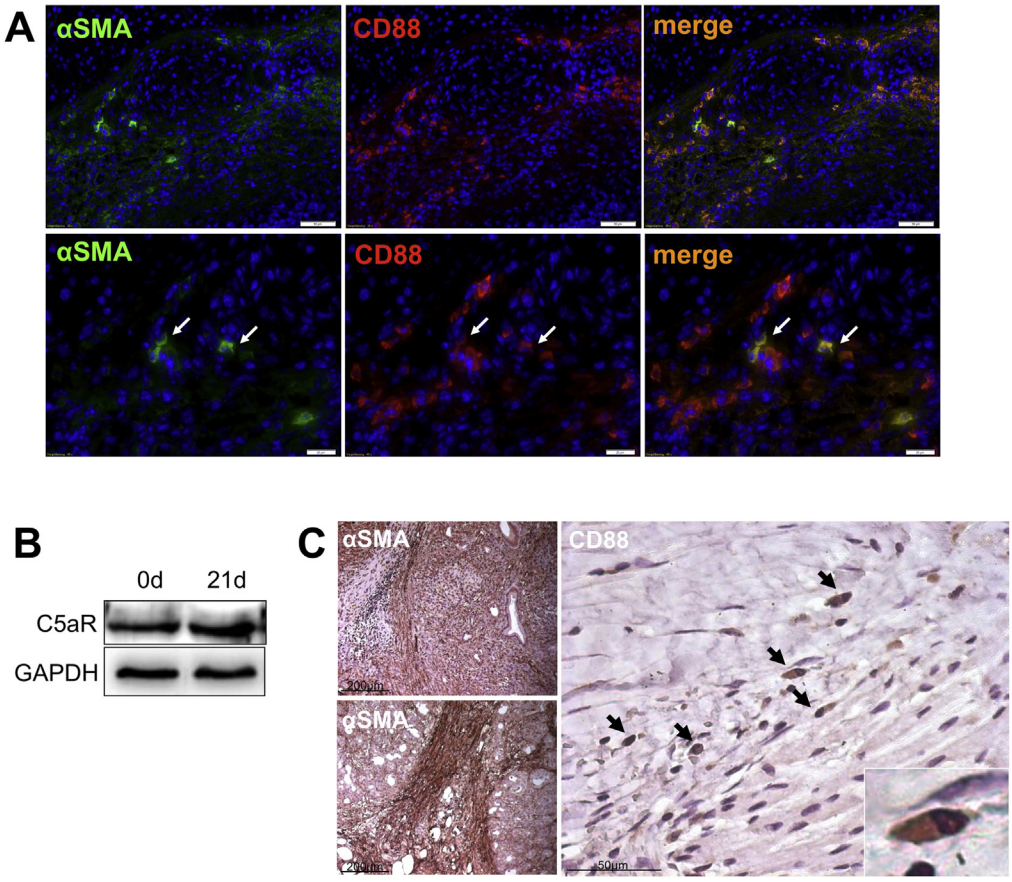

Figure 5. C5a-receptor expression on pancreatic stellate cells in chronic pancreatitis. (*A* and *B*) On immunofluorescence and Western blot analysis PSCs expressed CD88, the receptor of C5a as well as αSMA in pancreatic tissue of animals with chronic pancreatitis. Fluorescence staining indicated expression of CD88 on pancreatic stellate cells as well as on immune cells. (*C*) Human tissue samples of chronic pancreatitis patients showed a strong signal for αSMA and C5a (CD88) (n = 5–7). GAPDH, glyceraldehyde-3-phosphate dehydrogenase.

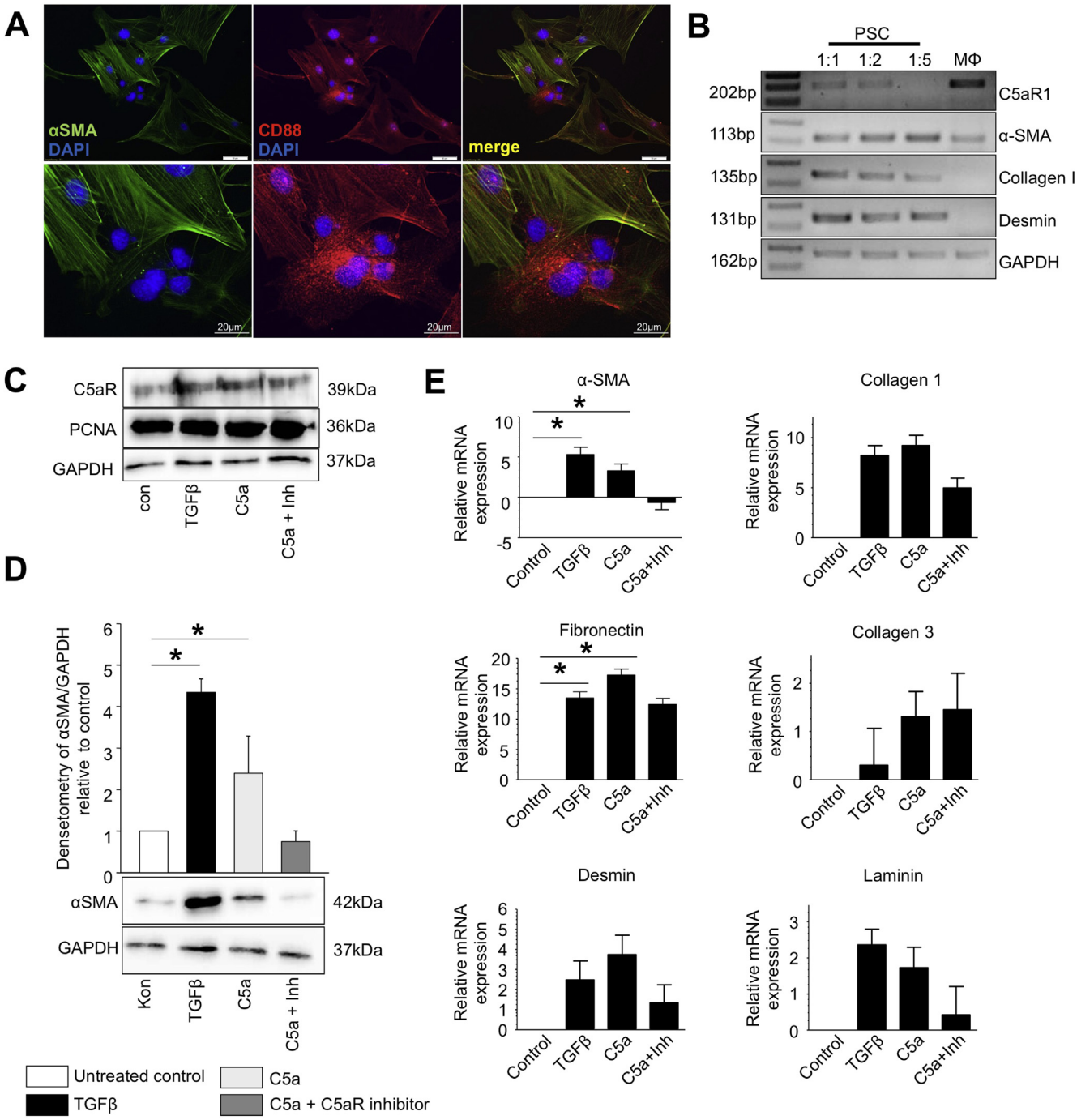

Figure 6. C5a activates PSCs in vitro, which leads to extracellular matrix deposition. Pancreatic stellate cells were isolated from C57Bl6 mice. (*A*) The expression of C5a receptor (CD88) on stellate cells was analyzed by immunofluorescence staining of isolated PSCs. (*B* and *C*) Reverse-transcription polymerase chain reaction as well as immunoblotting of PSC lysates confirmed positive immunofluorescence staining. (*C*) Proliferation shown by proliferating cell nuclear antigen (PCNA) Western blot was not affected by C5a stimulation. Murine PSCs express the C5a receptor and respond to recombinant mouse C5a with up-regulation of αSMA. (*D*) Four independent experiments were analyzed by Western blot and the ratio of αSMA/glyceraldehyde-3-phosphate dehydrogenase (GAPDH) optical density (OD) was calculated. (*E*) PSCs treated with C5a showed up-regulation of αSMA and fibronectin messenger RNA (mRNA) on real-time polymerase chain reaction analysis. TGFβ-stimulated and untreated cells acted as controls, a C5a-receptor antagonist was used to block stimulation (n = 4).

pancreas and therefore appropriate experimental models are warranted. Currently, there are 2 pathophysiological concepts: the first of these is based on the inflammation-necrosis-fibrosis sequence as the underlying pathogenic mechanism,[25,29] and the second concept focuses on the direct activation of pancreatic stellate cells via a pathologic stimulus.[30] In the first scenario the initial lesion starting the sequence is autodigestion by prematurely activated

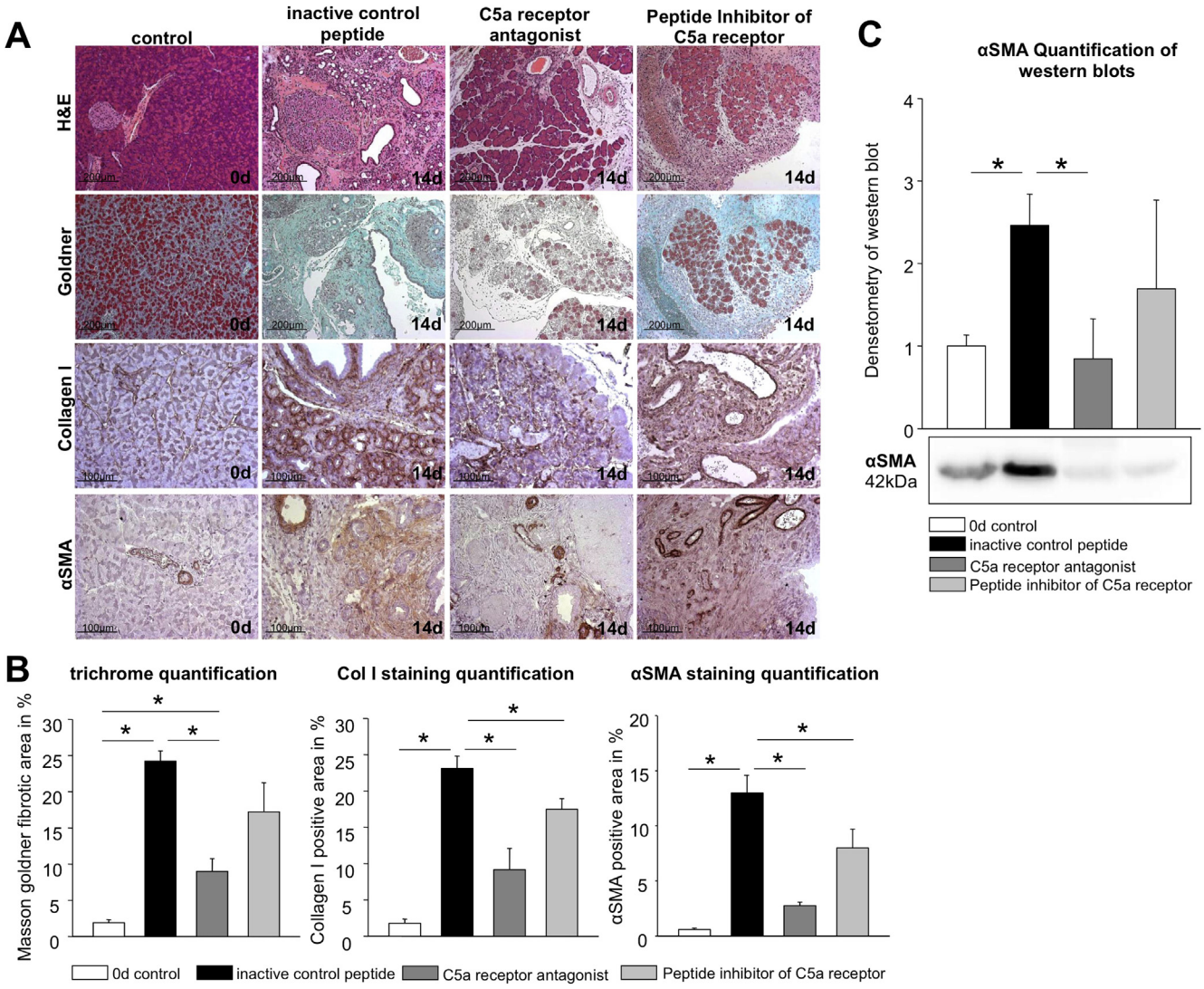

Figure 7. Treatment with C5a inhibitors attenuates fibrosis in the duct ligation model. Treatment with C5a-receptor antagonist and a peptide inhibitor of C5a was initiated 4 days after duct ligation and effects on fibrosis were evaluated after 14 days. (*A* and *B*) Both treatments lead to a significant reduction of Masson–Goldner, collagen I, and αSMA staining on histologic evaluation. (*C*) Western blot analysis for αSMA from pancreatic lysates confirmed this finding for the C5a-receptor antagonist and showed a similar trend that was not statistically significant for the peptide inhibitor (n = 6–9).

proteases. Our study aimed to combine these aspects. We established an animal model in which protease activation, systemic inflammation, and acinar cell necrosis are the starting points of chronic pancreatitis and in which we can show that the proinflammatory cytokine C5, most likely activated via proteolytic cleavage by pancreatic proteases, directly acts on PSCs and thus promotes fibrogenesis.

Repetitive cerulein application twice weekly over a period of 10 weeks, the model used here as pancreatitis control, is the most widely used model of chronic pancreatitis in mice.[31] It causes collagen deposition, which regresses when injections are discontinued. Combined lipopolysaccharide and ethanol application, an established rat model of chronic pancreatitis injury, has not been tested in mice, and dibutyl-tin-chloride is unsuited for experiments in mice because of differences in pancreatic and bile duct anatomy between rodents.[32] The model developed and characterized in this study includes a number of characteristic features observed in human disease and thus shows advantages over previous models: (1) progressive tissue destruction, activation of stellate cells, and exocrine tissue replacement by extracellular matrix after a single injury; (2) duct dilatation and duct plugging; (3) a strong inflammatory reaction and tissue regeneration; and (4) nerve sprouting combined with marked pancreatic pain. However, by design, the model only affects part of the pancreas, which has the advantage that each animal can serve as its own histologic control and that exocrine and endocrine function are preserved, therefore allowing long-term studies. Furthermore, this model offers the opportunity to use different genetically engineered mice in a highly reproducible setting.

To study fibrogenesis in chronic pancreatitis we investigated the role of C5. Our study showed a direct effect of C5

on the development of fibrosis in 2 separate models of chronic pancreatitis.

The complement system represents a part of the innate immune system, which is involved in bacterial defense and attracts neutrophils and macrophages to the site of inflammation. It is well established that activation of inflammatory cells determines the severity of pancreatitis.[33] To our surprise, the deletion of C5 did not result in decreased inflammation or a reduced severity of acute pancreatitis. Reports in the literature on this aspect are controversial. Although Merriam et al[34] reported a less severe phenotype of pancreatitis in C5-deficient mice, Bhatia et al[27] observed an increase in severity with a more pronounced inflammatory response in *C5*-deleted animals. In our setting we found no effect of an influence of C5 deletion on the severity of acute pancreatitis. A possible explanation for this finding could be the compensation of C5a by other proinflammatory cytokines or chemokines such as monocyte chemoattractant protein-1, IL6, or TNFα.[35,36]

With regard to fibrogenesis our data differed completely and suggested that parenchymal necrosis is the initiator of fibrosis, and that the extent of fibrogenesis is determined by the presence of C5a. C5a was found to play an important role in liver fibrosis by stimulating HSCs.[10] HSCs express the C5a receptor on their surface and a direct activating effect of C5a on HSCs has been reported.[37,38] PSCs are related closely to HSCs.[8] PSCs are responsible for the production of extracellular matrix proteins and tissue fibrosis during chronic pancreatitis. The activation of PSCs is mediated by a plethora of different cytokines such as IL6, TNFα, TGF-β, and IL10,[4,7,39] and results in an increased expression of αSMA. In addition to the activation of PSCs within the pancreas, their progenitor cells migrate from bone marrow into the pancreas. C5a appears to play a role as a direct activator of PSCs as well as a chemokine for PSC progenitor cells or the recruitment of inflammatory cells into the pancreas and to promote fibrosis. Our experiments show that C5a can activate PSCs in vivo and in vitro. This suggests a similar pathophysiological mechanism behind the profibrotic function of C5a in liver disease and pancreatitis. Activation of the complement system by pancreatic proteases such as trypsin[16,40] may start recovery from pancreatic necrosis by induction of fibrosis through activating PSCs.

Whether or not variants of the human C5 gene represent risk factors for fibrotic disease has been discussed controversially. The SNPs rs17611 and rs2300929 have been found to be associated with increased liver fibrosis in a small cohort reported by Hillebrandt et al,[10] but the results could not be replicated in a larger, multicenter confirmation study.[12] We therefore investigated the allele distribution of these *C5* SNPs in a prospectively recruited cohort of pancreatitis patients and found that none of these mutations was associated with an increased risk for acute or chronic pancreatitis when compared with healthy blood donors from the same area. However, the formerly reported risk alleles lead to increased transcription levels of C5 in a large population-based cohort. In context to our animal studies this observation indicated that previously reported risk alleles can predispose to higher circulating C5 levels and thus a more fibrogenic environment in pancreatitis.

Targeting PSCs and their profibrotic mediators would be a promising new therapeutic strategy to reduce fibrogenesis and disease progression in chronic pancreatitis. Previously, Emori et al[41] found that the serine protease inhibitor camostat reduces fibrogenesis in a rat model of chronic pancreatitis, an effect that could be mediated via the complement cascade. However, the use of broad-spectrum serine protease inhibitors in chronic disease could be burdened with a number of side effects. Our finding that direct blockage of C5aR1 by a small-molecule inhibitor in a therapeutic setting reduces the progression of chronic pancreatitis suggests that pharmacologic inhibition of C5 may represent a valid therapeutic approach. Eculizumab, a Food and Drug Administration–approved therapeutic antibody blocking C5 activation, could be a promising agent for testing in randomized clinical trials.[42]

In conclusion, we have identified C5 in 2 models of chronic pancreatitis as a drugable mediator of pancreatic fibrosis that directly activates pancreatic stellate cells and whose deletion or inhibition greatly reduces fibrogenesis after pancreatic necrosis.

Supplementary Material

Note: To access the supplementary material accompanying this article, visit the online version of *Gastroenterology* at www.gastrojournal.org, and at http://dx.doi.org/10.1053/j.gastro.2015.05.012.

References

1. **Mayerle J, Hoffmeister A**, Werner J, et al. Chronic pancreatitis–definition, etiology, investigation and treatment. Dtsch Arztebl Int 2013;110:387–393.
2. Gress TM, Muller-Pillasch F, Lerch MM, et al. Balance of expression of genes coding for extracellular matrix proteins and extracellular matrix degrading proteases in chronic pancreatitis. Z Gastroenterol 1994;32:221–225.
3. Haber PS, Keogh GW, Apte MV, et al. Activation of pancreatic stellate cells in human and experimental pancreatic fibrosis. Am J Pathol 1999;155:1087–1095.
4. Mews P, Phillips P, Fahmy R, et al. Pancreatic stellate cells respond to inflammatory cytokines: potential role in chronic pancreatitis. Gut 2002;50:535–541.
5. Apte MV, Haber PS, Darby SJ, et al. Pancreatic stellate cells are activated by proinflammatory cytokines: implications for pancreatic fibrogenesis. Gut 1999;44:534–541.
6. Apte MV, Phillips PA, Fahmy RG, et al. Does alcohol directly stimulate pancreatic fibrogenesis? Studies with rat pancreatic stellate cells. Gastroenterology 2000;118:780–794.
7. **Schneider E, Schmid-Kotsas A**, Zhao J, et al. Identification of mediators stimulating proliferation and matrix synthesis of rat pancreatic stellate cells. Am J Physiol Cell Physiol 2001;281:C532–C543.
8. Buchholz M, Kestler HA, Holzmann K, et al. Transcriptome analysis of human hepatic and pancreatic stellate cells:

organ-specific variations of a common transcriptional phenotype. J Mol Med (Berl) 2005;83:795–805.
9. Friedman SL. Mechanisms of hepatic fibrogenesis. Gastroenterology 2008;134:1655–1669.
10. Hillebrandt S, Wasmuth HE, Weiskirchen R, et al. Complement factor 5 is a quantitative trait gene that modifies liver fibrogenesis in mice and humans. Nat Genet 2005; 37:835–843.
11. Hillebrandt S, Goos C, Matern S, et al. Genome-wide analysis of hepatic fibrosis in inbred mice identifies the susceptibility locus Hfib1 on chromosome 15. Gastroenterology 2002;123:2041–2051.
12. Halangk J, Sarrazin C, Neumann K, et al. Evaluation of complement factor 5 variants as genetic risk factors for the development of advanced fibrosis in chronic hepatitis C infection. J Hepatol 2008;49:339–345.
13. Roxvall L, Bengtson A, Heideman M. Anaphylatoxin generation in acute pancreatitis. J Surg Res 1989;47:138–143.
14. Roxvall LI, Bengtson LA, Heideman JM. Anaphylatoxins and terminal complement complexes in pancreatitis. Evidence of complement activation in plasma and ascites fluid of patients with acute pancreatitis. Arch Surg 1990;125:918–921.
15. **Halangk W, Lerch MM**, Brandt-Nedelev B, et al. Role of cathepsin B in intracellular trypsinogen activation and the onset of acute pancreatitis. J Clin Invest 2000; 106:773–781.
16. Acioli JM, Isobe M, Kawasaki S. Early complement system activation and neutrophil priming in acute pancreatitis: participation of trypsin. Surgery 1997;122:909–917.
17. Olson LM, Moss GS, Baukus O, et al. The role of C5 in septic lung injury. Ann Surg 1985;202:771–776.
18. Sumichika H, Sakata K, Sato N, et al. Identification of a potent and orally active non-peptide C5a receptor antagonist. J Biol Chem 2002;277:49403–49407.
19. **Kourtzelis I, Rafail S**, DeAngelis RA, et al. Inhibition of biomaterial-induced complement activation attenuates the inflammatory host response to implantation. FASEB J 2013;27:2768–2776.
20. **Schwaiger T, van den Brandt C**, Fitzner B, et al. Autoimmune pancreatitis in MRL/Mp mice is a T cell-mediated disease responsive to cyclosporine A and rapamycin treatment. Gut 2014;63:494–505.
21. Apte MV, Haber PS, Applegate TL, et al. Periacinar stellate shaped cells in rat pancreas: identification, isolation, and culture. Gut 1998;43:128–133.
22. Guenther A, Aghdassi A, Muddana V, et al. Toll-like receptor 4 polymorphisms in German and US patients are not associated with occurrence or severity of acute pancreatitis. Gut 2010;59:1154–1155.
23. **Mayerle J, den Hoed CM, Schurmann C**, et al. Identification of genetic loci associated with Helicobacter pylori serologic status. JAMA 2013;309:1912–1920.
24. Kloppel G, Maillet B. The morphological basis for the evolution of acute pancreatitis into chronic pancreatitis. Virchows Arch A Pathol Anat Histopathol 1992; 420:1–4.
25. Erkan M, Adler G, Apte MV, et al. StellaTUM: current consensus and discussion on pancreatic stellate cell research. Gut 2012;61:172–178.
26. Ceyhan GO, Bergmann F, Kadihasanoglu M, et al. Pancreatic neuropathy and neuropathic pain–a comprehensive pathomorphological study of 546 cases. Gastroenterology 2009;136:177–186 e1.
27. Bhatia M, Saluja AK, Singh VP, et al. Complement factor C5a exerts an anti-inflammatory effect in acute pancreatitis and associated lung injury. Am J Physiol Gastrointest Liver Physiol 2001;280:G974–G978.
28. Krizhanovsky V, Yon M, Dickins RA, et al. Senescence of activated stellate cells limits liver fibrosis. Cell 2008; 134:657–667.
29. Detlefsen S, Sipos B, Feyerabend B, et al. Fibrogenesis in alcoholic chronic pancreatitis: the role of tissue necrosis, macrophages, myofibroblasts and cytokines. Mod Pathol 2006;19:1019–1026.
30. Vonlaufen A, Phillips PA, Xu Z, et al. Withdrawal of alcohol promotes regression while continued alcohol intake promotes persistence of LPS-induced pancreatic injury in alcohol-fed rats. Gut 2011;60:238–246.
31. Aghdassi AA, Mayerle J, Christochowitz S, et al. Animal models for investigating chronic pancreatitis. Fibrogenesis Tissue Repair 2011;4:26.
32. Lerch MM, Gorelick FS. Models of acute and chronic pancreatitis. Gastroenterology 2013;144:1180–1193.
33. Sendler M, Dummer A, Weiss FU, et al. Tumour necrosis factor alpha secretion induces protease activation and acinar cell necrosis in acute experimental pancreatitis in mice. Gut 2013;62:430–439.
34. Merriam LT, Webster C, Joehl RJ. Complement component C5 deficiency reduces edema formation in murine ligation-induced acute pancreatitis. J Surg Res 1997;67:40–45.
35. **Zhang H, Neuhofer P**, Song L, et al. IL-6 trans-signaling promotes pancreatitis-associated lung injury and lethality. J Clin Invest 2013;123:1019–1031.
36. Zhou GX, Zhu XJ, Ding XL, et al. Protective effects of MCP-1 inhibitor on a rat model of severe acute pancreatitis. Hepatobiliary Pancreat Dis Int 2010;9: 201–207.
37. Schlaf G, Schmitz M, Heine I, et al. Upregulation of fibronectin but not of entactin, collagen IV and smooth muscle actin by anaphylatoxin C5a in rat hepatic stellate cells. Histol Histopathol 2004;19:1165–1174.
38. **Xu R, Lin F**, He J, et al. Complement 5a stimulates hepatic stellate cells in vitro, and is increased in the plasma of patients with chronic hepatitis B. Immunology 2013; 138:228–234.
39. **Michalski CW, Gorbachevski A**, Erkan M, et al. Mononuclear cells modulate the activity of pancreatic stellate cells which in turn promote fibrosis and inflammation in chronic pancreatitis. J Transl Med 2007;5:63.
40. Lasson A, Laurell AB, Ohlsson K. Correlation among complement activation, protease inhibitors, and clinical course in acute pancreatitis in man. Scand J Gastroenterol 1985;20:335–345.
41. Emori Y, Mizushima T, Matsumura N, et al. Camostat, an oral trypsin inhibitor, reduces pancreatic fibrosis induced by repeated administration of a superoxide dismutase inhibitor in rats. J Gastroenterol Hepatol 2005;20: 895–899.

42. **Greinacher A, Friesecke S**, Abel P, et al. Treatment of severe neurological deficits with IgG depletion through immunoadsorption in patients with Escherichia coli O104:H4-associated haemolytic uraemic syndrome: a prospective trial. Lancet 2011;378:1166–1173.

Author names in bold designate shared co-first authorship.

Received April 7, 2014. Accepted May 12, 2015.

Reprint requests
Address requests for reprints to: Julia Mayerle, MD, Department of Medicine A, University Medicine, Ernst-Moritz-Arndt-University, Greifswald, Ferdinand-Sauerbruchstrasse, 17475 Greifswald, Germany. e-mail: mayerle@uni-greifswald.de; fax: (49) 3834-86-7234.

Acknowledgments
The authors gratefully acknowledge the excellent technical assistance of Mrs Kathrin Gladrow and Mrs Diana Kühl.

Conflicts of interest
The authors disclose no conflicts.

Funding
Supported by the Deutsche Krebshilfe/Dr Mildred Scheel-Stiftung (109102), the Deutsche Forschungsgemeinschaft (DFG GRK840-D2/E3/E4, MA 4115/1-2/3, WA 2430/2-1), the Federal Ministry of Education and Research (BMBF GANI-MED 03IS2061A, and BMBF 0314107, 01ZZ9603, 01ZZ0103, 01ZZ0403, and 03ZIK012), the MTA-SZTE Momentum grant (LP2014-10/2014), and the European Union (EU-FP-7: EPC-TM and EU-FP7-REGPOT-2010-1).

Supplementary Material and Methods

Materials

Cerulein was obtained from Sigma (Taufkirchen, Germany). Human MPO was from Calbiochem (San Diego, CA). The elastase substrate R110-(CBZ-Ala-Ala) was obtained from Invitrogen (Eugene, OR). The Amyl amylase quantification kit as well as the Lip lipase quantification kit were purchased from RocheHitachi (Grenzach-Whylen, Germany). Recombinant mouse TGFβ1 was obtained from Cell Signaling Technology (Danvers, MA) and recombinant mouse C5a was obtained from Hycultec (Beutelsbach, Germany). All other chemicals of highest purity were obtained either from Sigma-Aldrich (Eppelheim, Germany), Merck (Darmstadt, Germany), Amersham Pharmacia Biotech (Buckinghamshire, UK), or Bio-Rad (Hercules, CA). The C5a-receptor antagonist (W-54011) was obtained from Calbiochem.[1] Peptide inhibitor for C5a receptor AcF-(OpdChaWR) as well as inactive control peptide AcdChaPWFRO-NH_2 characterized by Kourtzelis et al,[2] were synthesized by Biosyntan GmbH.

Animal Models

C57Bl6 mice were purchased from Charles River (Germany), breeder pairs of C5-deficient mice as well as C5 wild-type animals were purchased from Jackson Lab.[3] Chronic pancreatitis was induced by ligation of the pancreatic duct at the junction between the gastric and the duodenal lobe, sparing the bile duct and its concomitant artery in animals at the age of 8–10 weeks weighing approximately 25 g (Figure 1*A*). The animals received a single application of cerulein (50 μg/kg/body weight) 2 days after duct ligation. Animals were killed at 3, 7, 14, and 21 days after ligation. Inhibition of C5a receptor was performed by daily IP injections of C5a-receptor antagonist W-54011 (200 μg/kg/body weight) starting 4 days after duct ligation. Peptide inhibitor as well as inactive control peptide were injected daily intraperitoneally in a concentration of 10 μmol/L starting on day 4 after ligation. Animals were killed 14 days after pancreatic duct ligation.

A second model of chronic pancreatitis was induced by 6 IP injections of cerulein (50 μg/kg/body weight) twice a week over a time period of 10 weeks. The animals were killed 2 days after the last course of injection. Acute pancreatitis was induced by 8-hourly IP injection of supramaximal concentrations of cerulein (50 μg/kg/body weight). All animals were starved overnight with access to water ad libitum.

Open field analysis for measurement of pancreatic pain was performed in a 50 $\times$ 50 cm square box, as described by Cattaruzza et al.[4] Voluntary movement of mice was detected by a camera and distances of movement were analyzed with ImageJ software. All animal experiments were performed after prior approval by the institutional animal care committee.

Histology, Immunohistochemistry, and Immunofluorescence

Pancreatic tissue, lung, and liver from killed animals were fixed immediately in 4% formalin for paraffin embedding. Paraffin sections were used for H&E staining and Masson–Goldner staining. Antigen retrieval of paraffin sections for immunohistochemistry was performed with Target Retrieval Solution (Dako). Fibrosis was detected by collagen I staining (rabbit polyclonal, cat no. ab292; Abcam), proliferation was assessed by nuclear localization of Ki67 (rabbit polyclonal, cat no. IHC-00375; Bethyl), and stellate cells were detected by αSMA staining (mouse monoclonal clone 1A4; Sigma-Aldrich). Infiltrating macrophages were detected by anti–Mac-3 antibody (rat monoclonal, clone M3/84; BD Pharmingen), and differentiation between M1 and M2 macrophages was performed by fluorescence labeling of the M1 population by CD68 (antibody online, cat no. ABIN181836) and of the M2 population by CD206 (antibody online, cat no. ABIN1386219) in cryo sections of the pancreas. Neutrophils were labeled with anti-MPO antibody (polyclonal rabbit, cat no. ab45977; Abcam). Anti-protein gene product 9.5 (rabbit polyclonal, ref. Z5116; Dako) was used to stain pancreatic nerves. Intact β-cells were labeled with anti-insulin (4590; Cell Signaling). Anti–cytokeratin 19 (polyclonal rabbit, cat no. ab15463; Abcam) was used to label ductal structures. Antibodies were used in a dilution of 1:50 up to 1:1000 in Aureon bovine serim (Wageningen, The Netherlands) albumin or 20% fetal calf serum.

Oil red staining was generated by the Oil Red O Stain Kit (IHC World), Masson–Goldner staining was performed with the Masson–Goldner staining Kit (Merck, Darmstadt, Germany). Quantification of Goldner staining and immunohistochemistry was performed using ImageJ and expressed as a percentage of area staining positive for collagen I, insulin, and αSMA staining (Supplementary Figure 1).

Immunofluorescence staining in cryosections of pancreatic tissue was used to localize C5a receptor (CD88). Sections were fixed in ice-cold methanol/acetone. CD88 antibody (rat monoclonal, cat no. 135804; BioLegend) was used in a dilution of 1:100 in Aureon bovine serum albumin. Anti–α-amylase (sc-46657; Santa Cruz) was used to mark intact secretory tissue.

For immunofluorescence staining of PSCs, cells were cultured on chamber slides, fixed with 4% formalin, permeabilized with 0.1% Triton X, and blocked using 1% bovine serum albumin. CD88 antibody (antibodies online, rabbit polyclonal, cat no ABIN272007) and αSMA antibody were used in 1:200 in 1% bovine serum albumin.

Biochemical Assays

Serum levels of amylase and lipase were measured by photometric assay (Roche Hitachi). Purified enzymes (Sigma) were used as standard. Elastase in feces was determined by fluorometric enzyme kinetic over 1 hour at 37°C using rhodamine-110-CBZ-Ala-$Ala_{(2)}$ (Invitrogen, Karlsruhe, Germany) as substrate dissolved in 100 mmol/L Tris containing 5 mmol/L $CaCl_2$ at pH 8.0. Feces were resuspended in 500 mmol/L NaCl, 100 mmol/L $CaCl_2$ charged with 0.1% Triton X-100, and sonicated. For measurements of MPO, pancreatic tissue was homogenized on ice in 20 mmol/L potassium phosphate buffer (pH 7.4) and

centrifuged. The pellet was resuspended in 50 mmol/L potassium phosphate buffer (pH 6.0) containing 0.5% cetyltrimethylammoniumbromide. The suspension was freeze-thawed in cycles, sonicated, and centrifuged at 20,000*g*. MPO activity was assayed in 50 mmol/L potassium phosphate buffer (pH 6) containing 0.53 mmol/L O-dianisidine and 0.15 mmol/L H_2O_2. The initial increase in absorbance was measured at room temperature with a Spectramax spectrophotometer (Molecular Devices, Biberach, Germany). The results are expressed in units of MPO activity. Cytokines were measured by fluorescence-activated cell sorter analysis with cytometric bead array from Becton Dickinson (mouse inflammation kit, cat: 552364; Heidelberg, Germany).[5]

Western Blot Analysis

Tissue samples or plated PSCs for Western blot experiments were homogenized on ice in lysis buffer containing 25 mmol/L HEPES (pH 7.5), 75 mmol/L NaCl, 0.5% Triton X-100, 5% glycerol, and 1 mmol/L EDTA in the presence of different protease inhibitors (10 mmol/L NaF, 5 mmol/L Na4P2O7, 1 mmol/L phenylmethylsulfonyl fluoride, and 1 mg/mL aprotinine). Protein content was determined by the Bradford assay or BCA kit from Pierce (Rockford, IL). In all, 10- to 50-mg samples of total protein were loaded on 12.5% polyacrylamide gels and transferred to nitrocellulose membranes for immunoblotting. αSMA antibody (Sigma Aldrich), CD88 antibody (Santa Cruz), and mouse anti-PCNA (Invitrogen, Carlsbad, CA) were used at a dilution of 1:1000, anti–glyceraldehyde-3-phosphate dehydrogenase (mouse monoclonal, clone 6C5; Meridian, Memphis, TN) was used as loading control. Densitometry for αSMA was performed using ImageJ software and dividing optical density of αSMA bands by the optical density of the glyceraldehyde-3-phosphate dehydrogenase band after background subtraction.

Pancreatic Stellate Cell Isolation

Stellate cells were isolated from murine pancreas by collagenase digestion and Nycodenz density gradient centrifugation (Nycomed Pharma, Oslo, Norway). This method was established previously and described by Apte et al.[6] The pancreata of 4–5 mice were pooled to get enough cells for the experimental setting. PSCs were maintained in Iscove's modified Dulbecco's medium (Life Technologies, Grand Island, NY) containing 10% heat-inactivated fetal calf serum and PenStrep. Cells were used before the first passage.

Polymerase Chain Reaction and Real-Time Polymerase Chain Reaction Analysis of Isolated Stellate Cells

Total RNA from PSCs was isolated using the RNeasy mini kit and transcribed into complementary DNA using the Quantitect RT kit from Qiagen (Hilden, Germany). Reagents for regular polymerase chain reaction were from PAN Biotech (Aidenbach, Germany). Real-time polymerase chain reaction was conducted on a 7500 real-time polymerase chain reaction system using Sybr Select Master Mix from Life Technologies (Austin, TX). All primers were from Invitrogen (Darmstadt, Germany): C5aR1: F-5'-ACTTCCTT CAGAAGAGTTGCCT-3', R-5'-AATGCCATCCGCAGGTATGT-3'; αSMA: F-5'-GCCAGTCGCTGTCAGGAACCC-3', R-5'-CCAGC GAAGCCGGCCTTACA-3'; collagen I: F-5'-AGGCCACGCAT GAGCCGAAG-3', R-5-GCCATGCGTCAGGAGGGCAG-3'; collagen 3: F-5'-AGGATCTGAGGGCTCGCCAGG-3', R-5'-AGCCA CCAGACTTTTCACCTCCA-3'; fibronectin: F-5'-GCCTGAGG TGGACCCCGCTA-3', R-5'-GGGCCCAAGTGACCCGCATC-3'; desmin: F-5'-TAGACGACCTGCAGAGGCT-3', R-5'-GCGCTCCA GGTCAATACGAG-3'; glyceraldehyde-3-phosphate dehydrogenase: F-5'-CCCCAGCAAGGACACTGAGCAA-3', R-5'-GTGGG TGCAGCGAACTTTATTGATG-3'; laminin: F-5'-GGACGGGA ATTCCGTTAGGG-3', R-5'-TTGTAGGTCAAAGGCTCGGC-3'; and Rpl32: F-5'-AACCCAGAGGCATTGACAAC-3', R-5'-CACC TCCAGCTCCTTGACAT-3'.

C5 SNP Analysis in Human Patients With Pancreatitis

Blood samples from patients with pancreatitis admitted to Greifswald University Medicine were collected after informed consent and ethics committee approval[7,8] and healthy blood donors prospectively were collected, anonymized, and DNA was isolated from leukocytes using samples centrifuged at 3000 rpm for 10 minutes. Genomic DNA was extracted from the cell pellets using the DNA isolation kit I from Magna Pure LC (initial cohort; Roche Diagnostics, Indianapolis, IN) or the Quick-gDNA MiniPrep Kit (follow-up study; Zymo Research, Irvine, CA). For SNP analysis only acute pancreatitis of a nonbiliary and non–endoscopic retrograde cholangiopancreatography etiology, and for chronic disease only alcohol-induced or idiopathic pancreatitis, were included. TaqMan assays C_11720402_10 for the SNP rs17611 and C_2783669_1 for SNP rs2300929 purchased from Life Technologies (Grand Island, NY) were used for genotyping. TaqMan products were verified by direct sequencing.

Expression of Quantitative Trait Loci Analysis of Candidate SNPs

The Study of Health in Pomerania is a longitudinal population-based cohort study in West Pomerania, a region in northeast Germany, assessing the prevalence and incidence of common population-relevant diseases and their risk factors. Baseline examinations for the Study of Health in Pomerania–TREND were performed between 2008 and 2012, comprising 4420 participants. Study design and sampling methods were reported previously.[9] The present expression of quantitative trait loci analysis was based on a subset of 976 subjects aged 20–81 years from the Study of Health in Pomerania–TREND study population for which genome-wide SNP typing data as well as genome-wide whole-blood gene expression data were available.[2,8]

Statistical Analysis

All data are expressed as means ± SEM from at least 5 animals in each group. Statistical analyses were performed using Sigma-Plot for the animal experiments and Prism

(Statcon, Witzenhausen, Germany) for PSC experiments and human data. An unpaired, 2-tailed, Student *t* test was used for statistical analysis of in vivo and in vitro experiments and the Fisher exact test was used for human C5 SNP analysis. Differences were considered significant at a level of a *P* value less than .05.

References

1. Sumichika H, Sakata K, Sato N, et al. Identification of a potent and orally active non-peptide C5a receptor antagonist. J Biol Chem 2002;277:49403–49407.
2. **Kourtzelis I, Rafail S**, DeAngelis RA, et al. Inhibition of biomaterial-induced complement activation attenuates the inflammatory host response to implantation. FASEB J 2013;27:2768–2776.
3. Olson LM, Moss GS, Baukus O, et al. The role of C5 in septic lung injury. Ann Surg 1985;202:771–776.
4. Cattaruzza F, Johnson C, Leggit A, et al. Transient receptor potential ankyrin 1 mediates chronic pancreatitis pain in mice. Am J Physiol Gastrointest Liver Physiol 2013;304:G1002–G1012.
5. **Schwaiger T, van den Brandt C**, Fitzner B, et al. Autoimmune pancreatitis in MRL/Mp mice is a T cell-mediated disease responsive to cyclosporine A and rapamycin treatment. Gut 2014;63:494–505.
6. Apte MV, Haber PS, Applegate TL, et al. Periacinar stellate shaped cells in rat pancreas: identification, isolation, and culture. Gut 1998;43:128–133.
7. Guenther A, Aghdassi A, Muddana V, et al. Toll-like receptor 4 polymorphisms in German and US patients are not associated with occurrence or severity of acute pancreatitis. Gut 2010;59:1154–1155.
8. Whitcomb DC, Muddana V, Langmead CJ, et al. Angiopoietin-2, a regulator of vascular permeability in inflammation, is associated with persistent organ failure in patients with acute pancreatitis from the United States and Germany. Am J Gastroenterol 2010;105:2287–2292.
9. Völzke H, Alte D, Schmidt CO, et al. Cohort profile: the study of health in Pomerania. Int J Epidemiol 2011;40:294–307.

Author names in bold designate shared co-first authorship.

Supplementary Table 1. Allele Frequency of C5 SNPs rs17611 and rs 2300929 in Patients With Pancreatitis

	Chronic pancreatitis		Acute pancreatitis			Blood donors		
	n	%	n	%	*P*	n	%	*P*
rs17611								
n	390		133			384		
AA	84	21.5385	23	17.2932		76	19.7917	
AG	183	46.9231	75	56.391		197	51.3021	
GG	123	31.5385	35	26.3158		111	28.9063	
A	351	45	121	45.4887		349	45.4427	
G	429	55	145	54.5113	.9431	419	54.5573	.8783
rs2300929								
n	390		133			384		
TT	311	79.7436	104	78.1955		310	80.7292	
TC	77	19.7436	27	20.3008		68	17.7083	
CC	2	0.51282	2	1.50376		6	1.5625	
T	699	89.6154	235	88.3459		688	89.5833	
C	81	10.3846	31	11.6541	.5668	80	10.4167	1.0000

Supplementary Table 2. Demographic Data of Cohorts for SNP Analysis

	Chronic pancreatitis	Acute pancreatitis		Blood donors	
			P		*P*
Median age, *y*	45	47	.2802	33	<.0001
Female	24.17%	26.32%	.5603	45.57%	<.0001

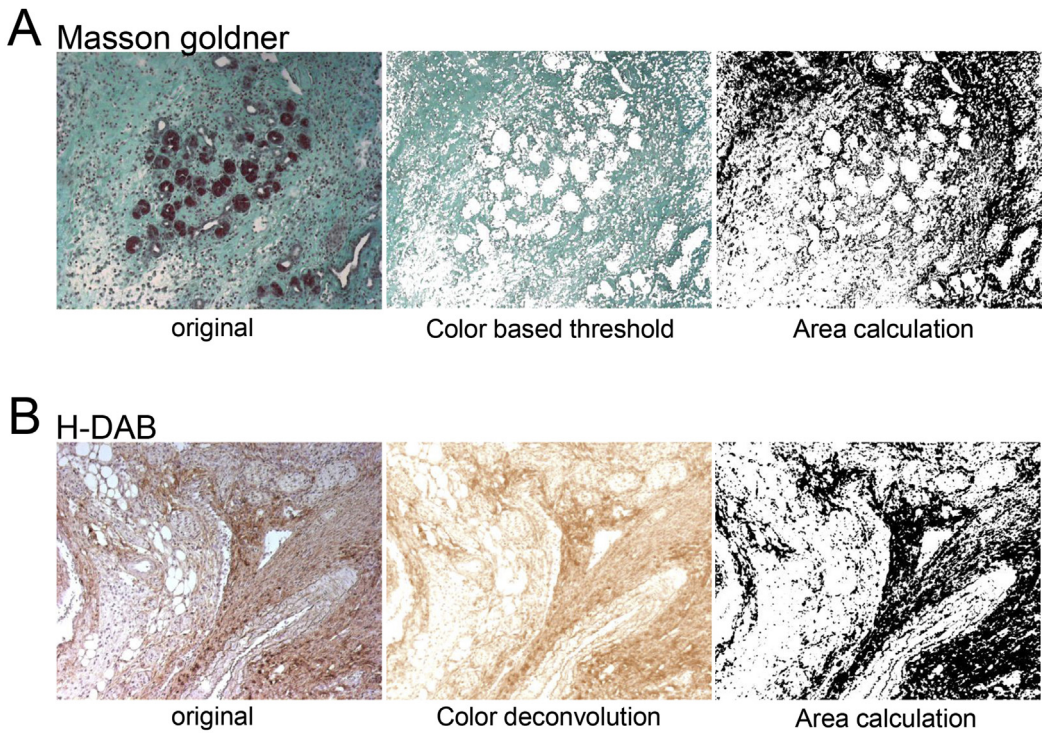

Supplementary Figure 1. Quantification of fibrosis by ImageJ software. ImageJ is used for the quantification of fibrosis from Masson–Goldner trichrome staining or haematoxylin-3,3′-diaminobenzidine (H-DAB) staining or a respective protein such as αSMA or collagen I.

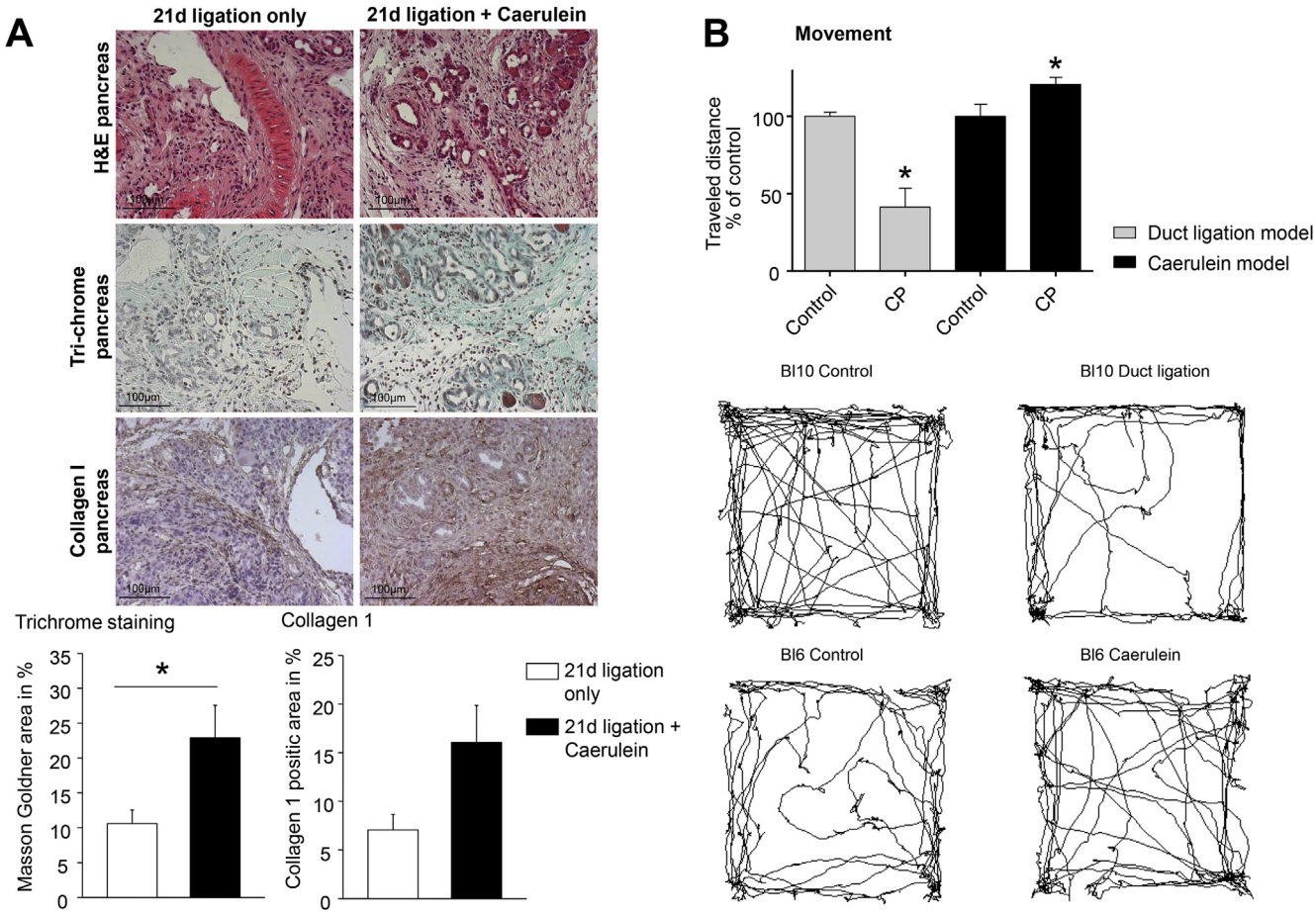

Supplementary Figure 2. Pancreatic duct ligation without cerulein hyperstimulation and open field analysis in animals with chronic pancreatitis (CP). (*A*) Pancreatic duct ligation without supramaximal cerulein stimulation served as control for the characterization of the model. In duct ligation alone we observed less extended areas of necrosis (H&E staining), less fibrosis (trichrome staining, collagen I), a less-pronounced inflammatory infiltrate, but atrophy of the gland over time. Morphometric quantification of fibrosis on Masson–Goldner trichrome staining and collagen I shows a significant increase in extracellular matrix in duct-ligated, cerulein-stimulated animals compared with ligation without cerulein stimulations. Interestingly, open field analysis to measure pancreatic pain showed a significant decrease in traveled distance in the duct ligation/hyperstimulation model in comparison with repetitive cerulein application. (*B*) Voluntary movement and the distance traveled by animals in the duct ligation/hyperstimulation. More than 5 animals were used for each experiment and all experiments were performed in triplicate. All experiments were performed independently on 3 or more occasions. Asterisks indicate significant differences with a *P* value less than .05.

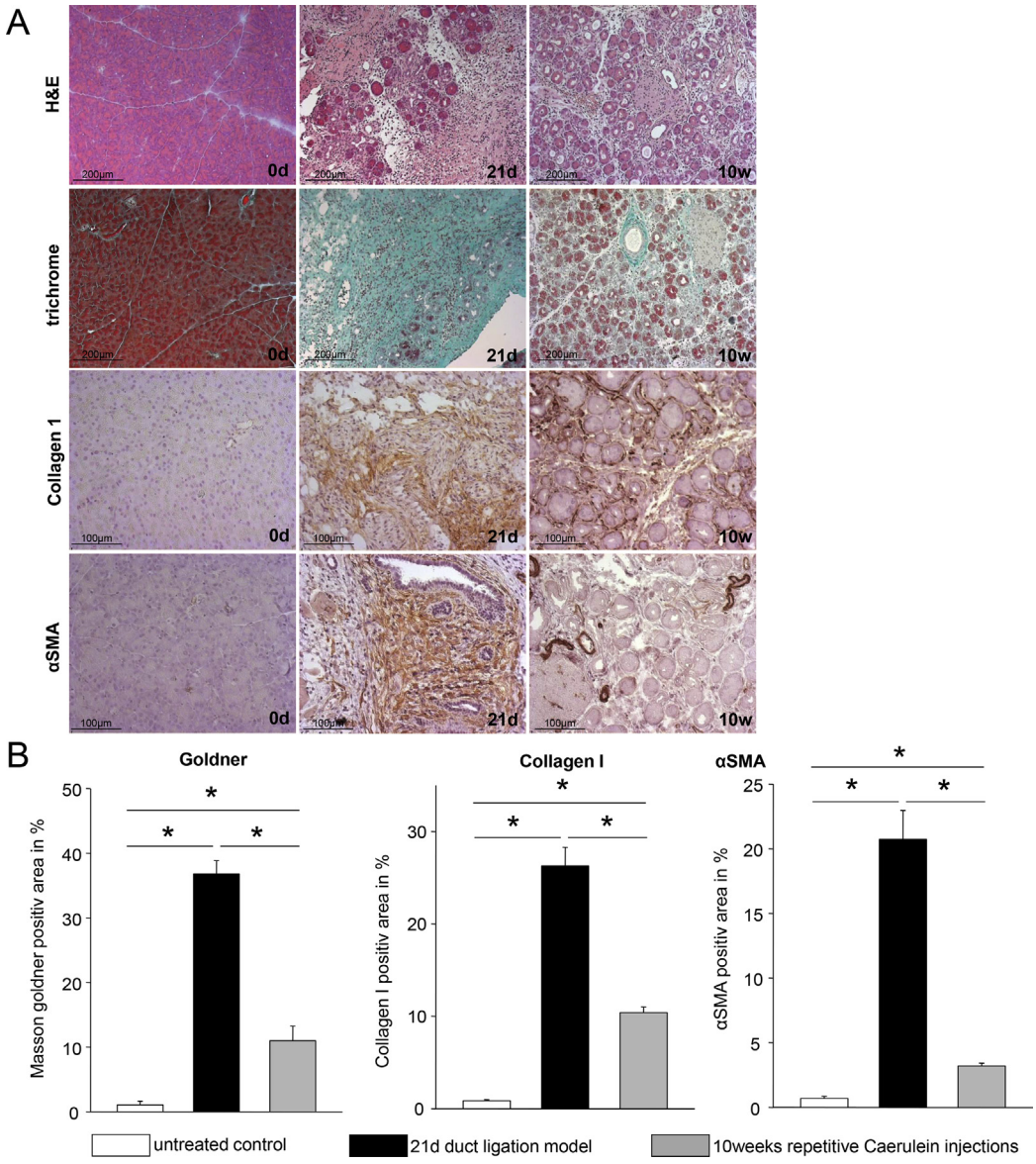

Supplementary Figure 3. Direct comparison of the duct ligation/hyperstimulation model to repetitive supraphysiological cerulein injections with regard to fibrogenesis. (*A* and *B*) Morphometric quantification of fibrosis on Masson–Goldner trichrome staining, collagen I, and αSMA staining showed a highly significant difference of fibrosis between the duct ligation model at day 21 and after 10 weeks of repetitive cerulein stimulation. More than 5 animals were used for each experiment and all experiments were performed in triplicate. All experiments were performed independently on 3 or more occasions. Asterisks indicate significant differences with a *P* value less than .05.

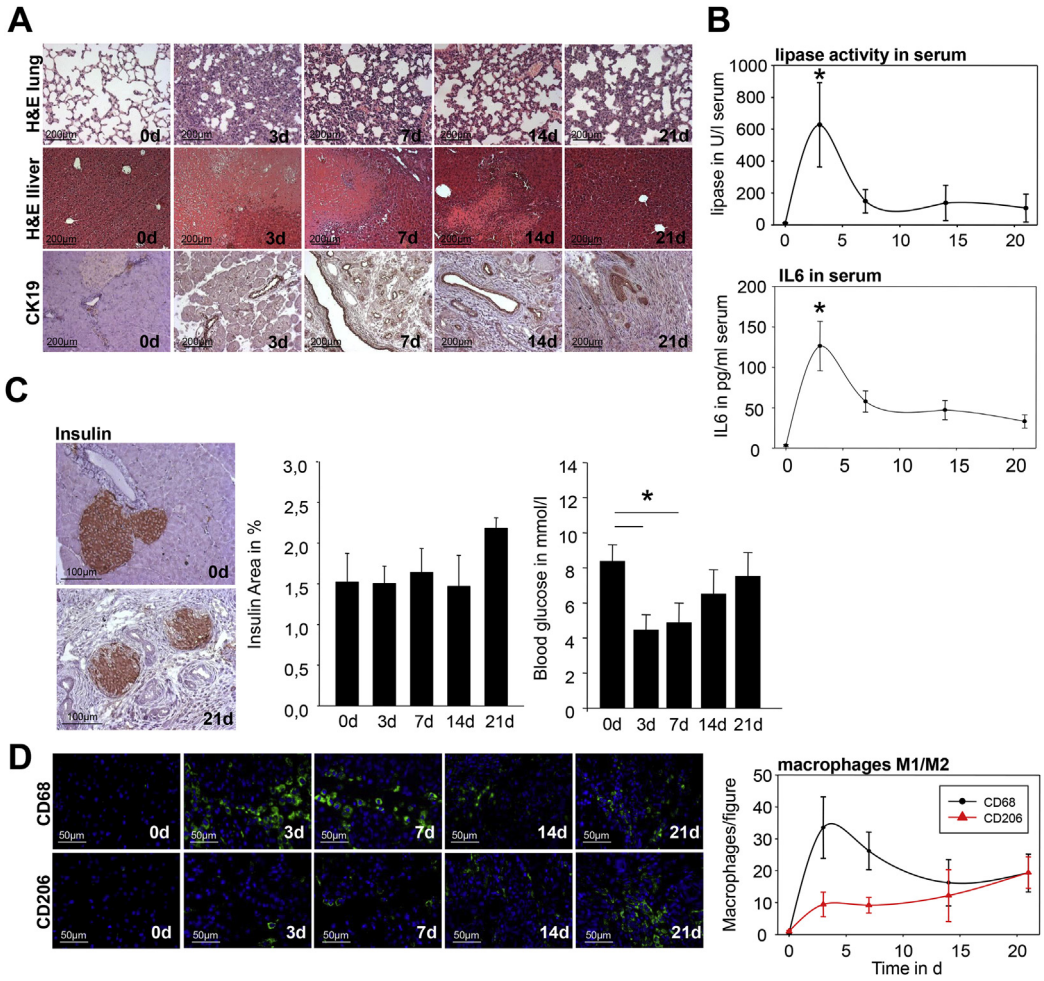

Supplementary Figure 4. Further characterization of the duct ligation/hyperstimulation model in C57Bl6 mice. (*A*) H&E staining of the lungs of animals with chronic pancreatitis upon concomitant duct ligation and supramaximal secretagogue stimulation showed a strong systemic inflammatory reaction with thickening of the alveolar wall and hyperemia. H&E staining of the liver showed extended areas of necrosis at 3 and 7 days after surgery, which resolved at later time points, ruling out mechanical cholestasis as a confounding factor. Staining of cytokeratin 19 (CK19) illustrated strong expression of intact but dilated pancreatic ducts over the time course of chronic pancreatitis. (*B*) Time course of serum lipase activity and IL6 serum levels in chronic pancreatitis in the duct ligation model. (*C*) Staining of insulin over the time course of chronic pancreatitis in mice showed unchanged numbers of insulin-producing cells and, after a dip in the early necrotizing disease phase, a preserved endocrine function in the duct-ligated mouse model. Quantification of the M1 and M2 populations of macrophages showed a predominance of the proinflammatory M1 macrophages in the early disease course, peaking at day 3 in pancreatic tissue. (*D*) Thereafter, a steady increase in M2 macrophages, which are considered responsible for extracellular matrix deposition in the later course of chronic pancreatitis, was observed. Asterisks indicate significant differences with $P < .05$.

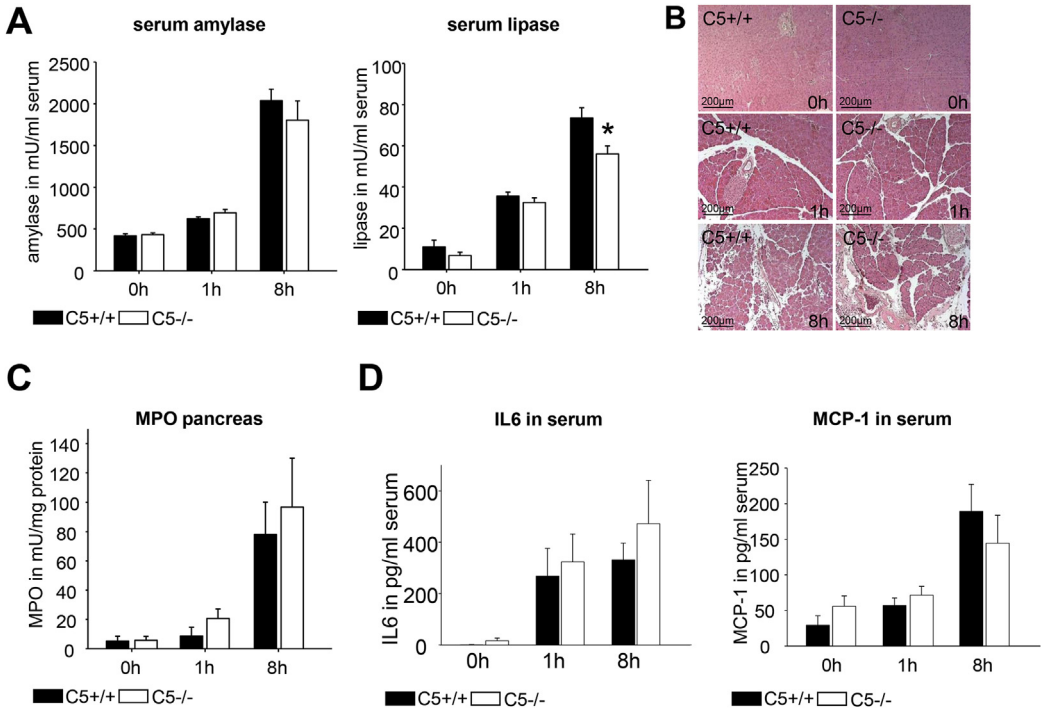

Supplementary Figure 5. C5 in cerulein-induced pancreatitis. Acute pancreatitis was induced by supramaximal cerulein administration (50 μg/kg/body weight) in C5+/+ and C5-/- animals. (*A*) Serum amylase and lipase activity showed an increase after induction of pancreatitis, but amylase and lipase activities were not found to be different between the 2 animal strains. (*B*) Representation of H&E stainings at 0, 1, and 8 hours of repetitive cerulein IP injection in C5+/+ compared with C5-/- animals; 0h represents untreated control. H&E staining of the pancreas showed an equal amount of infiltrating cells as well as equal levels of tissue damage characterized by areas of necrosis or edema. (*C*) Myeloperoxidase activity in pancreatic tissue homogenate was found to be increased over time but did not differ between C5+/+ and C5-/- animals. (*D*) Serum levels of the proinflammatory cytokine IL6 or the chemokine monocyte chemoattractant protein (MCP)-1 were not different between C5+/+ and C5-/- mice. More than 5 animals were used for each experiment and all experiments were performed in triplicate. All experiments were performed independently on 3 or more occasions. Asterisks indicate significant differences with a *P* value less than .05.

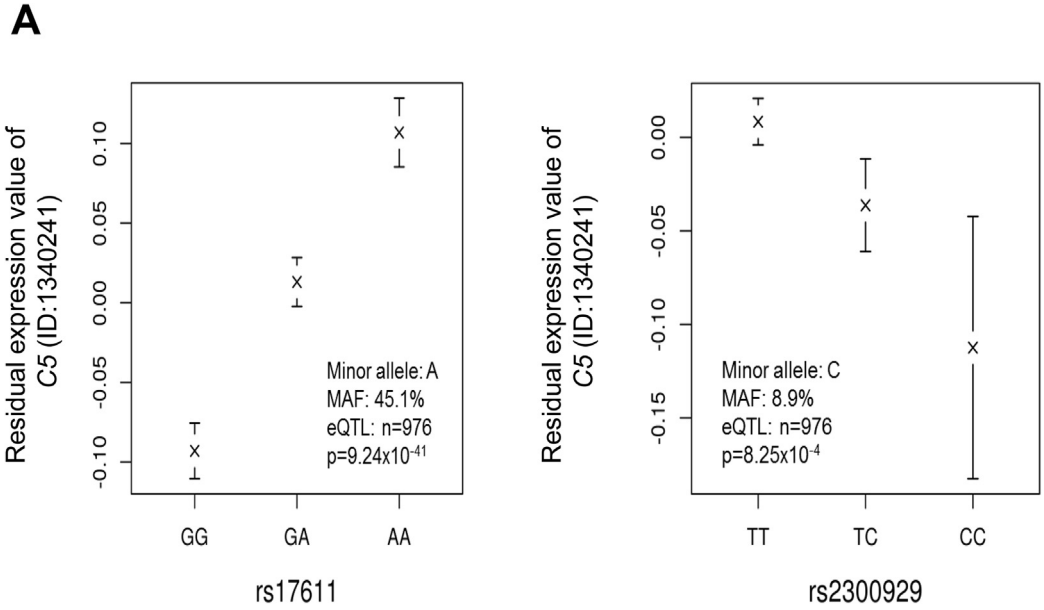

Supplementary Figure 6. Expression level of C5 in whole blood corresponding to the SNPs rs17611 and rs2300929. (*A*) Shown are the residual (ie, after adjustment for technical effects and potential confounders, and overall mean-centered) mean $\log_2$-transformed gene expression levels corresponding to gene-specific messenger RNA level in whole blood from a *cis*-expression of quantitative trait loci analysis of 976 volunteers from the Study of Health in Pomerania–Trend cohort and 95% confidence intervals (y-axis) per genotype group (x-axis) of *C5* adjusted for the first 50 eigenvectors with respect to rs17611 and rs2300929 for SHIP–TREND. We detected a significant association of rs17611_A with increased *C5* expression measured in whole blood with a *P* value of 6.87×10^{-41}.

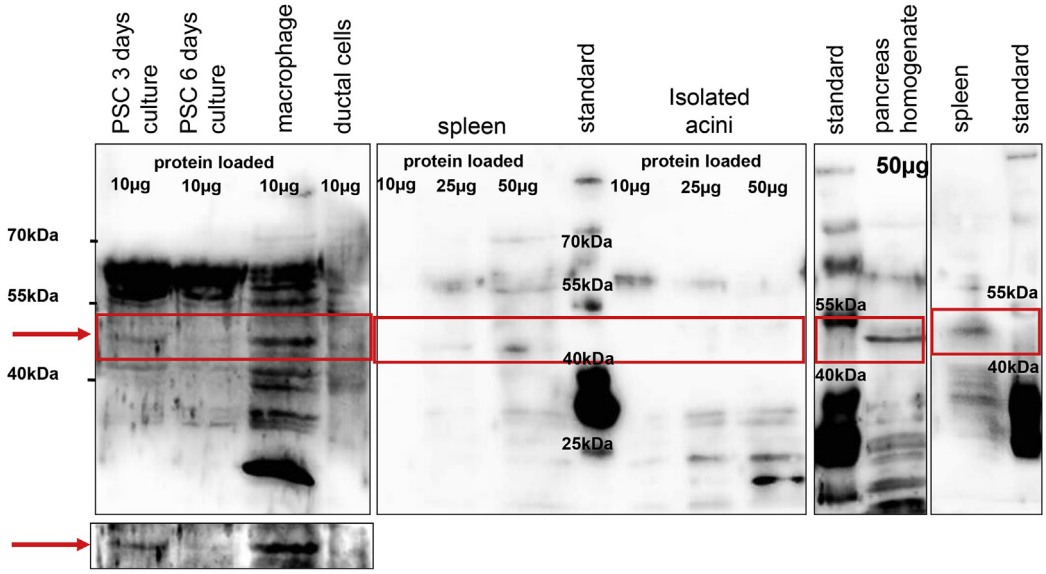

10% SDS gel, western blot of C5a receptor (Santa cruz sc-25774 rabbit polyclonal)
expected size ~49kDa

Supplementary Figure 7. Full-length Western blot for C5a receptor on pancreatic cells. Western blots of different pancreatic cells and tissues were preformed to analyze the expression of C5a receptor (CD88). The expected size of CD88 is approximately 49 kilodaltons. Isolated macrophages served as positive control. Freshly isolated PSCs (3 days of culture) show an expression of CD88 in Western blot. Long-time culture of PSCs (6 days) leads to activation of cells and loss of CD88 expression. Duct cells, similar to isolated acinar cells, do not express CD88, in contrast to whole pancreatic tissue, which shows a clear expression of CD88.

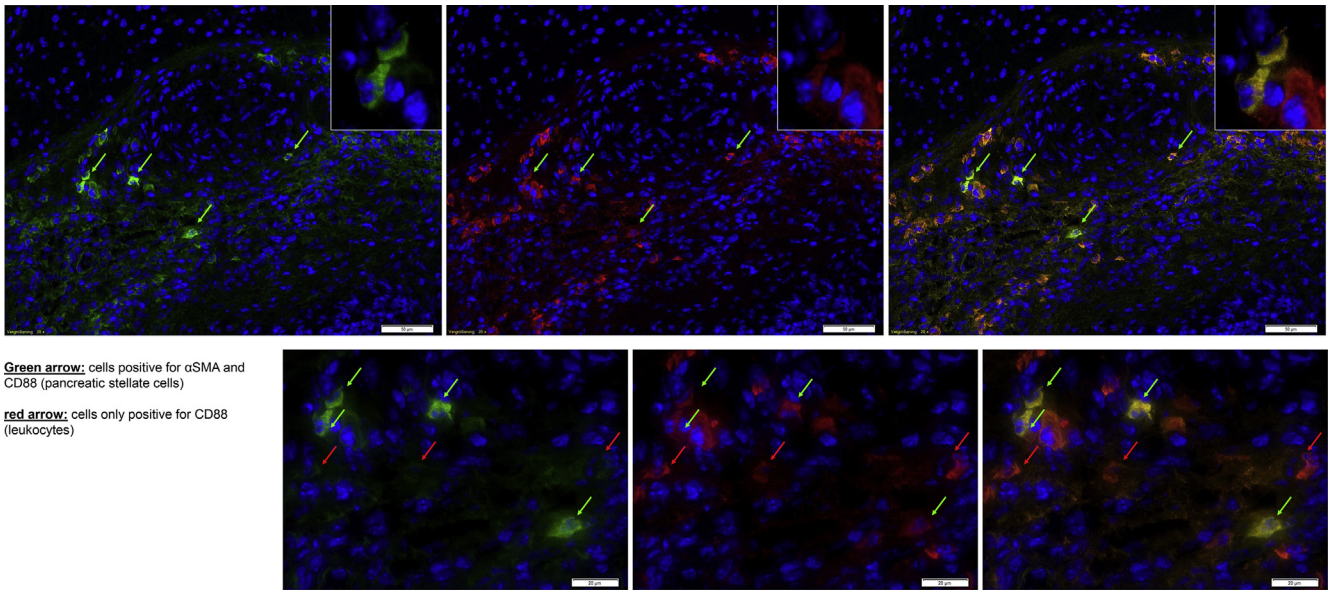

Supplementary Figure 8. Enlarged immunofluorescent staining of C5a receptor (CD88) and αSMA shows expression of CD88 in different populations of cells but not in acinar cells. In addition, CD88/αSMA double-positive cells can be stained in chronic pancreatitis tissue of mice, identifying them as PSCs.